VITAMIN D AND INNATE IMMUNITY IN PNEUMONIA AND COPD

THE UNIVERSITY OF
WAIKATO
Te Whare Wānanga o Waikato

A thesis
submitted in partial fulfilment
of the requirements for the degree
of
Master of Science in Biology
at
The University of Waikato
by
Talia Mary Simpson

_____

The University of Waikato
2010

Abstract

A resurgence of interest in vitamin D research has led to the discovery that it plays a role in an unexpectedly large number of biological processes, and that reduced levels of this hormone are implicated in a range of diseases. In fact, it is estimated that vitamin D is involved in the regulation of 3% of the human genome. Two genes containing the target sequence indicative of vitamin D regulation are those encoding LL-37 and hBD-2. These antimicrobial peptides are integral components of the innate immune system and act as natural antibiotics to help combat infection.

The respiratory epithelium exposes a large surface area to environmental pathogens, making the innate immune response extremely important in its defence. Microbial infection of the respiratory tract is the cause of pneumonia, and is implicated in cases of COPD exacerbation. This study aimed to determine whether a relationship existed between vitamin D, LL-37 and hBD-2 in 185 patients admitted to Waikato hospital with either condition. It was hypothesised that low vitamin D would correlate with reduced peptide levels, and that this would be associated with increased infection severity and higher mortality rates.

Peptide concentrations in patient plasma were measured by indirect ELISA and compared to 25D levels. Statistical analysis revealed no significant associations between vitamin D status, peptide levels and severity, but did show increased mortality in individuals with severe vitamin D deficiency or low LL-37.

Based on the significance of LL-37 as a predictor of mortality (particularly in COPD), development of a plasma screening method using MALDI-TOF mass spectrometry was attempted, as a potential means of identifying patients most at risk. The success of this method was limited however, as the low abundance and small size of the mature peptide caused detection problems.

A protocol for assessing the vitamin D binding protein (DBP) genotype was developed, as it influences baseline 25D levels and response to supplementation. The association between low vitamin D and mortality suggests that supplementation could improve survival rates and, as the supplement dose required for effectiveness is genotype-dependent, this method could allow determination of the appropriate amount to administer to at-risk individuals.

Acknowledgements

I would like to thank my supervisor Dr Ray Cursons for his help and encouragement throughout the year, particularly when nothing seemed to be working the way it should.

I would also like to thank everyone else in the C.2.03 and C.2.10 laboratories for their help, especially those who volunteered their DNA for my study. Thank you also for allowing me to hoard all the gel electrophoresis equipment and for listening to my complaints.

Thank you to Jonathan Puddick for his help with the mass spectrometry part of my project, and for answering my constant stream of questions.

The Respiratory department research team at Waikato Hospital – Dr Noel Karalus, Dr Leong Leow and Associate Professor Robert Hancox, thank you very much for agreeing to partake in this project and for your work on the hospital-based part of the study. Thanks also to Robert Hancox for his work on the statistics, and answering all my questions promptly and thoroughly.

Thanks also to the Waikato Medical Research Fund for supporting this project.

Finally, I would like to thank my friends and family for their support and general awesomeness – Mum, Dad, Amy, Dale, Downey, Scott, Caleb, Fahad, Melissa, Ztoiven, 'shloi – thank you, thank you, thank you!

Table of Contents

List of Figures

List of Tables

List of Abbreviations

1,25D	1,25-dihydrovitamin D_3
25D	25-hydroxyvitamin D_3
AB	Acrylamide:N,N'-Methylenebisacrylamide
ACN	Acetonitrile
AMP	Antimicrobial peptide
APS	Ammonium persulphate
bp	Base pairs
BSA	Bovine serum albumin
CAMP	Cathelicidin antimicrobial peptide gene
CAP	Community acquired pneumonia
CF	Cystic fibrosis
CHCA	α-Cyano-4-hydroxycinnamic acid
COPD	Chronic obstructive pulmonary disease
CURB65	Marker of infection severity based on confusion, urea concentration, respiration rate, blood pressure, and age
DBP	Vitamin D binding protein
DNA	Deoxyribonucleic acid
dNTP	Deoxynucleotide Triphosphate
DTT	Dithiothreitol
EDTA	Ethylene diamine tetra acetic acid
ELISA	Enzyme-linked immunosorbent assay
Gc	Group-specific component
GLB	Gel loading buffer
hBD	Human β-defensin
hCAP-18	Human cathelicidin antimicrobial peptide
HCl	Hydrochloric acid
HD	Human defensin
HNP	Human neutrophil peptide
HRP	Horseradish peroxidase
IL-1	Interleukin-1
LL-37	Mature cathelicidin peptide

LPS	Lipopolysaccharide
IU	International units
Da	Daltons
mA	Milliampere
MAF	Macrophage-activating factor
MALDI	Matrix-assisted laser desorption/ionisation
Me/Ac	Methanol/acetic acid precipitation method
MS	Mass spectrometry
NCBInr	National Center for Biotechnology Information nonredundant database
PAGE	Polyacrylamide gel electrophoresis
PBS	Phosphate buffered saline
PCR	Polymerase chain reaction
PEG	Polyethylene glycol
ppm	Parts per million
RXR	Retinoic X receptor
SAA1	Serum amyloid A protein
sDHB	Super DHB (2,5-dihydroxybenzoic acid with 10% 5-methoxysalicylic acid)
SDS	Sodium dodecyl sulphate
SNP	Single nucleotide polymorphism
TAE	Tris-acetate EDTA buffer
TCA	Trichloroacetic acid
TEMED	Tetramethylethylenediamine
TFA	Trifluoroacetic acid
TLR	Toll-like receptor
TNF-α	Tumour necrosis factor-α
TOF	Time-of-flight
UV	Ultraviolet
VDR	Vitamin D receptor
VDRE	Vitamin D response element

1. Introduction

1.1 Vitamin D

Often referred to as the "sunshine vitamin"[1], vitamin D is actually a hormone with a multitude of biological roles in the body[2]. The discovery of vitamin D has largely been linked to studies on the disease rickets, which was first described in the 5th Century, BC. Since then, observations that rickets is less common among rural children than those living in cities - particularly in areas of heavy pollution, led to the recognition that sunlight plays an important role in the prevention and treatment of the disease. The agent responsible for this protective effect was later identified as vitamin D[3].

The importance of vitamin D in bone health has therefore been known for some time, but an increasing number of studies are beginning to show that it also plays a role in a wide range of other processes, such as in reducing the risk of infection. Unlike most vitamins, which function as general immunological agents, vitamin D can act specifically, and appears to be an integral component of the immune system[4]. A 1932 paper[5] recognised that much of the time lost due to illness at an industrial company was as a result of common colds, and that regular doses of cod-liver oil (which contains both vitamins A and D) may help to reduce this. They also noted that their experiment spanned "the season of greatest prevalence of colds and minimum sunlight and resistance to colds"[5], indicating that even at this early date, a connection was made between sunlight, vitamin D and immunity.

1.1.1 Sources and synthesis

In humans, vitamin D can be obtained in two ways: through the diet, and by synthesis in the body[1; 3]. Some foods naturally contain vitamin D (e.g. oily fish), while others (e.g. some milks and cereals) are fortified with the vitamin. Dietary sources however, are generally only minor contributors to the net daily intake of vitamin D[1].

The main source of vitamin D is synthesis from a precursor called 7-dehydrocholesterol, which is present in the skin. This precursor absorbs solar ultraviolet radiation in the UVB range (280-320 nm)[6], and uses the energy obtained to undergo transformation and subsequent isomerisation. The resulting

compound, vitamin D_3, is released into the circulation where it is transported by the vitamin D-binding protein[1; 3].

Once in the bloodstream, both diet-derived and synthesised vitamin D_3 follow the same downstream pathway, involving two hydroxylation steps (Figure 1.1). The first of these, catalysed by 25-hydroxylase (CYP27A1), takes place in the liver and forms 25-hydroxyvitamin D_3 (25(OH)D or 25D), while the second, catalysed by 1α-hydroxylase (CYP27B1), is carried out in the kidneys and generates 1,25-dihydroxyvitamin D_3 (1,25(OH)$_2$D or 1,25D), the active metabolite[1; 3; 7].
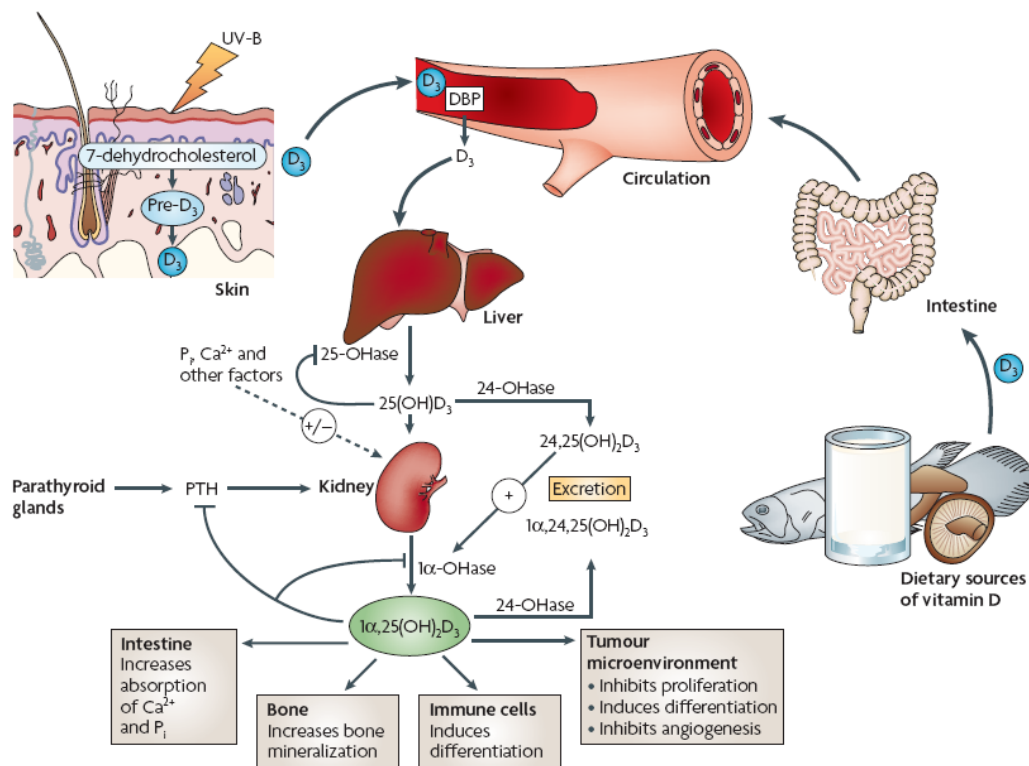
Figure 1.1 – Schematic representation of the synthesis and regulation of vitamin D, as published by Deeb et al.[8]

1.1.2   Factors influencing synthesis

Due to the fact that UVB radiation is required to catalyze the first step of the vitamin D synthesis pathway, any factor that influences the amount of UVB contacting the skin will also impact the capacity for vitamin D production. Such factors include: latitude, season, time of day, sunscreen use, skin pigmentation, culture and lifestyle. Additional factors, such as age, also have an effect[1; 3; 6].

i.   <u>Latitude, season and time of day</u>

Ultraviolet (UV) radiation travels to earth on an angle called the zenith angle, which is influenced by factors such as latitude, season and time of day. At smaller angles (i.e. lower latitudes, during summer, and between 10am and 3pm), the UV does not have as far to travel, and is therefore less likely to be absorbed by atmospheric molecules, such as ozone. Therefore, under these conditions, more UV will reach the earth surface, increasing the potential for vitamin D synthesis. For example, people living at the equator receive reasonably high levels of UV radiation all year round, while those at higher latitudes have lower levels. The amount of UV can be so low in these areas, particularly during winter, that little (if any) vitamin D can be synthesised[1; 6].

ii.   <u>Sunscreen use and skin pigmentation</u>

Sunscreen absorbs UVB photons, preventing them from entering the skin and catalysing vitamin D synthesis. Even low sun protection factor (SPF) sunscreens can block enough UV as to significantly reduce vitamin D production[1].

Melanin, the pigment that gives skin its colour, also absorbs UVB. Therefore, individuals with more of the pigment will produce less vitamin D than lighter-skinned individuals when exposed to the same amount of UV, for the same time[1]. This may explain why vitamin D deficiency is more common among darker-skinned groups[2; 9].

iii.   <u>Culture and lifestyle</u>

Cultural beliefs may influence vitamin D production[3]. For example, women in some cultures wear clothes over their entire body, significantly reducing their UVB-dependent vitamin D synthesis. Lifestyle choices (e.g. staying indoors) have a similar effect, which may explain why vitamin D levels are especially low in elderly and sick individuals[10; 11].

iv.   <u>Age</u>

Another explanation for the high prevalence of vitamin D deficiency in the elderly is the fact that older people have less 7-dehydrocholesterol in their skin, and therefore have a reduced capacity to produce vitamin D[1; 10; 11].

v.   Conflicting messages

Increased awareness about the dangers of UV, particularly in relation to skin cancer, has encouraged people to use sunscreen more often, and to seek shade or stay indoors between the hours of 10 am and 3 pm. While this does act to reduce the damaging effects of UV, it also limits vitamin D synthesis[1].

1.1.3   Vitamin D status

Although 1,25D is the active metabolite and carries out most of the roles associated with vitamin D, 25D is the main form present in the circulation and has a longer half-life. In addition, 1,25D can be produced in response to parathyroid hormone (PTH). The levels of this hormone rise during vitamin D deficiency, resulting in high serum 1,25D levels, which could confound the true vitamin D status of an individual. For these reasons, measurement of the 25D concentration in the circulation is the accepted means of determining vitamin D status[1; 3].

Vitamin D deficiency is defined as a serum 25D level of less than 20 ng/mL (50 nmol/L), while insufficient and sufficient vitamin D levels are classed as 20-32 ng/mL and >32 ng/mL, respectively[11]. The optimal level of vitamin D remains to be determined, and could lead to an increase in daily intake recommendations, which are currently: 200 IU/day for those aged <50 y; 400 IU/day for those 50-70 y; and 600 IU/day for those >70 y[1; 3; 11].

The belief that these intake guidelines need to be raised is supported by a number of studies. For example, it has been shown that a circulating vitamin D concentration of 30 ng/mL can be maintained with a daily intake of 500-1000 IU[11]. However, this exceeds the highest current daily recommended intake, while only producing vitamin D levels on the borderline of insufficiency and sufficiency.

Although a revision of daily adequate intake guidelines appears to be needed, determination of appropriate levels is difficult. Improved recommendations should not be supplied as an average for the general population, as this does not account for differences in an individual's place of residence (e.g. latitude), the time of year, or the personal characteristics of that individual (e.g. age, skin colour) - factors which have been shown to significantly impact vitamin D levels[3].

1.1.4   Mode of Action

1,25-dihydroxyvitamin D_3 (1,25D) exerts many of its biological effects via the nuclear vitamin D receptor (VDR), which consists of ligand- and DNA-binding domains. Upon entry to cells, 1,25D is transported to the nucleus where it binds in the ligand-binding domain of the VDR. This activates the receptor, allowing it to form a heterodimer with the retinoic X receptor (RXR). The DNA-binding domain allows the VDR-RXR complex to bind to specific repeat sequences on the DNA molecule, called vitamin D response elements (VDREs). This initiates the binding of a range of other proteins, and leads to the formation of a complex with the ability to regulate the expression of VDRE-containing genes. Vitamin D response elements are found in the regulatory regions of target genes, and although they are often in close proximity to gene promoters, they have also been found up to 75 kb away[9].

Vitamin D receptors have been identified in a wide range of cells, tissues and organs, including the brain, colon, prostate[3], breast, gonads, skin, pancreatic cells[1], bone[12], heart[1; 3], and many immune cells such as T lymphocytes and macrophages[9]. This suggests a widespread involvement of vitamin D in processes throughout the body. In fact, the vitamin D pathway is estimated to be involved in the regulation of 3% of the human genome[12].

1.1.5   Problems associated with deficiency

Vitamin D deficiency is not uncommon. Worldwide, estimated cases approach 1 billion, and the risk of deficiency is particularly high during winter, in individuals with dark skin, and in the elderly[13]. As vitamin D appears to be involved in such a wide range of physiological processes, it is not surprising that deficiency can result in a multitude of problems.

An increasing number of studies are showing correlations between vitamin D and a diversity of diseases, ranging from bone disorders (e.g. rickets[14]), to cancer, cardiovascular and autoimmune diseases (e.g. multiple sclerosis)[9]. Of particular interest to this study is the role of vitamin D in the immune response to infection, particularly with respect to the respiratory tract.

1.2   Antimicrobial peptides

Living organisms possess a wide range of defences to protect against microbial invasion, and these can be divided into innate and adaptive responses. The innate immune system is thought of as the "first line of defense"[15], and is relatively non-specific, but always active. This means it is able to act immediately upon invasion, but lacks the specificity of the adaptive response (e.g. antibody production)[16].

One innate mechanism is the production of antimicrobial peptides (AMPs). These are small (15-45 amino acid) peptides, usually with a net positive charge. They can be found in many organisms, including invertebrates, and have many features which are conserved across these species[17].

The antibiotic activity of these peptides makes them candidates for future therapeutic drugs, especially since some have been shown to have activity against bacterial strains which are resistant to antibiotics currently in use[15; 18]. These peptides have also been shown to have a range of other functions besides direct microbial killing, making their role in the immune system even more important than initially realised[15].

1.2.1   Mode of action

Antimicrobial peptides (AMPs) have been detected in many bodily fluids and secretions, such as blood, saliva, semen and sweat, and in a wide range of cells throughout the body. Expression by the epithelial cells of the skin, airways, gastrointestinal and genitourinary tracts, allow AMPs to function as a barrier for the host, by intercepting pathogens at surfaces in direct contact with the environment[15; 17; 18].

These peptides have also been found in immune cells such as lymphocytes and monocytes, where they may act as chemoattractants for other immune cells, allowing up-regulation of the immune response at the site of infection[15; 18]. Other immune cell-associated AMPs play a role in the elimination of phagocytosed microorganisms, as in the case of the α-defensins present in azurophil granules of neutrophils[15].

Most antimicrobial peptides are thought to kill their targets by the disruption of cell membranes, and the basic structural aspects shared by most

AMPs aid in this mechanism of action. The net positive charges of the peptides attract them to the negatively-charged bacterial membranes, and their amphipathic nature facilitates insertion[15; 17; 18]. This leads to leakage of cell contents and cell lysis, and must occur quickly to combat the rapid multiplication rate of bacteria[17].

Bacteria are not the only target however, as AMPs can also act on other microorganisms that possess membranes, including enveloped viruses (e.g. human immunodeficiency virus, HIV) and some fungi[15]. To make this process selective for invading microorganisms and prevent self-damage to the host, AMPs do not attack membranes containing cholesterol, which is a principal component of eukaryotic cells[17].

Homeostatic levels of natural host flora can be maintained by the constitutive expression of some AMPs, while inducible expression acts to increase protection during infection[17].

1.2.2   Classes

Antimicrobial peptides can be grouped into three main classes based on their structure. The first group contains peptides which do not have cysteine residues, so form linear α-helical structures (e.g. human cathelicidin, LL-37); the second includes peptides with cysteine residues arranged to form intramolecular disulphide bonds to give a β-sheet structure (e.g. human defensins); and peptides with a high proportion of a particular amino acid, such as arginine or proline, make up the third main group of antimicrobial peptides[17; 18].

In 2003, Boman[17] stated that "defensins and LL-37 are the components most essential for protecting our adult life from bacterial infections". Additionally, LL-37 has been found to act synergistically with the β-defensins[19], and the genes encoding LL-37 and human β defensin-2 (hBD-2) peptides contain VDREs[9]. In accordance with these findings, the focus of this study will be on the cathelicidin and defensin peptide families, and in particular, LL-37 and hBD-2.

1.3   Human cathelicidin

Members of the cathelicidin family of antimicrobial peptides are characterised by an N-terminal region with a sequence akin to that of cathelin. This region, referred to as the cathelin-like domain, is highly conserved between

species. Such conservation is made even more remarkable when compared to the C-terminal antimicrobial domain, which varies not only between, but also within species. This is the case in many species (e.g. cattle, pigs), where a number of different cathelicidin peptides have been identified. Even the ancient hagfish has two cathelicidin genes, indicating that these peptides have been conserved across many generations. However, a few organisms, including mice and humans, have only a single cathelicidin gene each[19; 20].

The importance of this peptide and its proper regulation in humans is evident in patients with morbus Kostmann. These individuals lack LL-37 due to a genetic disorder, and their condition is fatal without treatment[20].

1.3.1   Structure and processing

The human cathelicidin gene contains four exons, and is located on chromosome three[21]. Exons 1-3 hold the information for the signal sequence and cathelin-like domain, while the antimicrobial region is encoded by exon 4 (Figure 1.2). The product of this gene is a prepropeptide. After removal of the signal sequence, the propeptide hCAP-18 (human cathelicidin antimicrobial peptide) is produced[20].

Figure 1.2 – Basic structures of the human cathelicidin gene and precursor, modified from Ulrich et al.[20]

Much of the cathelicidin synthesised in myeloid cells is targeted for storage in the granules of neutrophils[22], but hCAP-18 has also been identified in a

wide range of body fluids (e.g. plasma, saliva), and epithelia (e.g. gut, respiratory tract)[17; 18; 19]. This epithelial expression can be induced in response to appropriate stimuli, and is often up-regulated during disease[20; 23].

In healthy individuals, hCAP-18 can be found in plasma at concentrations of 1.2-1.8 μg/mL. Retention of such levels would be damaging to the host if not for a factor in plasma that inhibits the antimicrobial and cytotoxic effects of the peptide[24]. Wang *et al.*[25] identified this factor as apolipoprotein A-I, a 28 kDa protein that sequesters cathelicidin by binding to the antimicrobial region (LL-37), probably through interactions similar to those involved in binding to bacterial membranes.

When the body is invaded by foreign organisms, inactive hCAP-18 can be converted to the mature peptide, which exhibits antimicrobial activity. This activation occurs when proteinase-3 cleaves off the cathelin-like domain[26]. The mature cathelicidin peptide produced is called LL-37, because it is 37 amino acid residues in length and begins with two Leucines, as shown in Figure 1.3[20].

LLGDFFRKSK-EKIGKEFKRI-VQRIKDFLRN-LVPRTES

Figure 1.3 – Amino acid sequence of LL-37

The cationic nature of this peptide is evident when examining the ratio of positive to negative charges in the sequence, which add up to give a net charge of +6, at physiological pH[20].

1.3.2   Actions

The actions of LL-37 can be separated into two broad groups: antimicrobial and signalling. The antimicrobial role of LL-37 is extremely important for the maintenance of adequate host protection, and is an integral part of the innate immune response. However, the activities of LL-37 are now known to extend past this, to a signalling role, where it may help to activate or enhance the adaptive immune response[20].

i.   Direct antimicrobial activity

The human cathelicidin peptide has direct antimicrobial activity against a wide range of microorganisms, including Gram-positive and -negative bacteria, as well as some fungi and enveloped viruses[19]. As shown in Figure 1.4, it is thought to exert this antibiotic effect by binding to bacterial membranes, possibly forming a carpet-like layer which disrupts the membrane and leads to the formation of pores[23; 27]. This would cause leakage of cell contents and lysis of the invading organism, and may occur at epithelial surfaces or within phagocytic cells[19].
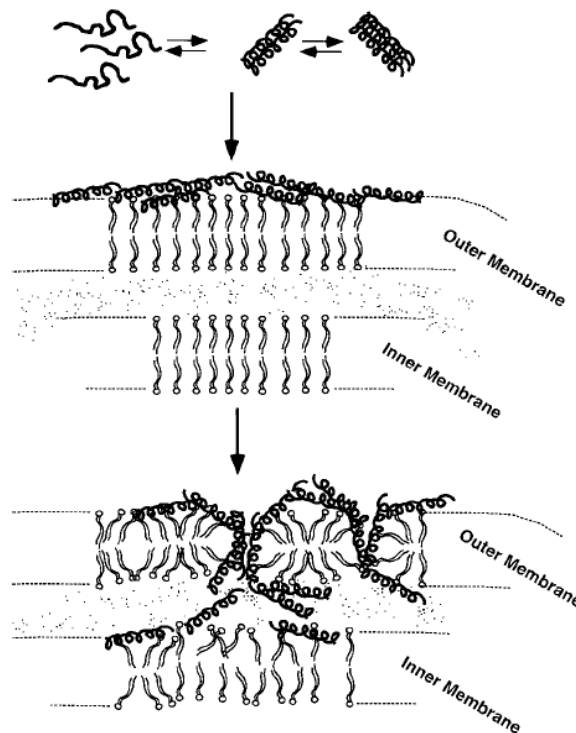
Figure 1.4 – Model of a possible mechanism of action for LL-37 on bacterial membranes, as published by Oren *et al.*[27]

Physiological conditions seem to induce aggregation of LL-37, leading to oligomerization, but it is unclear whether the oligomers or monomers interact with the membranes[20].

ii.   Other actions

A number of other roles have also been suggested for LL-37. For example, it can act as a chemoattractant, to recruit T cells and leukocytes (e.g. neutrophils and monocytes) to infected areas. It can also stimulate the release of proinflammatory mediators from mast cells, and increase expression of

chemokines and their receptors, which leads to further recruitment of cells to the infected or inflamed site[20; 28].

Due to this ability to promote inflammation, the expression of LL-37 must be regulated to prevent an uncontrolled response. It is therefore important to note that this peptide can also regulate the expression of anti-inflammatory genes, and can itself bind to bacterial lipopolysaccharide (LPS) and neutralise it[29]. LPS is released from bacterial cell membranes when they lyse, and can cause the production of proinflammatory agents such as tumour necrosis factor- α (TNF-α), leading to endotoxemia (or 'septic shock')[20; 28]. Cirioni *et al.*[29] showed that LL-37 was more effective at reducing plasma LPS and TNF-α levels than the β-lactams commonly used to treat septic shock.

These functions place LL-37 on the borderline of adaptive immunity, and may help to target this aspect of the immune response to the appropriate site[20; 23]. Based on its involvement in such a wide range of processes, it is not surprising that this peptide is so essential to host survival.

1.4   Human defensins

Like the cathelicidin family, defensins can be found in a wide range of species, both vertebrate and invertebrate[28], and this conservation shows the importance of these peptides in host defence[30]. Unlike the cathelicidins however, humans have many defensins, rather than just one, and they are separated into two subgroups: α-defensins and β-defensins[28].

Human defensin genes are found in a cluster on chromosome 8[31], but each subgroup is regulated differently[32]. Like the cathelicidins, both α- and β-defensin subfamilies are synthesised as precursor proteins, with a signal sequence, proregion, and antimicrobial domain (Figure 1.5). These precursors are processed to release the mature antimicrobial peptides[21].
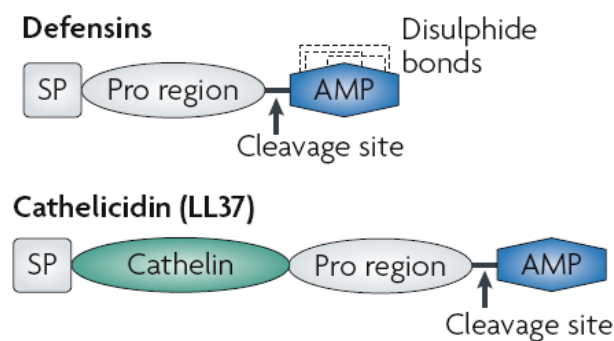
Figure 1.5 – Basic structural comparison of defensin and cathelicidin precursors, as published by Kolls *et al.*[30]

The mature peptides of both subgroups contain six cysteine residues, characteristic of defensins. This means that, although there is little homology between their primary sequences, they fold to form very similar β-sheet structures via the formation of three intramolecular disulphide bonds. Despite these structural similarities, there are several key features that distinguish each group. Firstly, the α-defensins are generally smaller, with 29-35 residues, as opposed to the 36-42 residues of the β-defensins. In addition, the cysteine pairings differ in each group, with bonds forming between cysteines 1-6, 2-4, and 3-5 in the α-defensins, and 1-5, 2-4, and 3-6 in the β-defensins[15; 18].

Another variation between the two classes is their location within the body. Human α-defensins are primarily found in the azurophil granules of neutrophils, where they are responsible for the killing of phagocytosed microorganisms. Based on this, they are often referred to as human neutrophil peptides (HNP 1-4), and are

synthesised in myeloid cells during neutrophil development. Two other α-defensins (HD 5-6) are found in the granules of Paneth cells in the small intestine[18; 31; 32]. This containment inside granules is necessary for α-defensins, because they are toxic to the host[17].

The β-defensins on the other hand are much more widespread, and have been found in epithelial cells throughout the body[18]. Each β-defensin peptide has a different distribution, and varies in whether it's expression is constitutive (e.g. hBD-1) or inducible[31].

The defensin that is the focus of this study, hBD-2 is found particularly in the skin, as well as in lung and tracheal epithelia, where it is thought to play a role in defending the airway mucosa. Expression of hBD-2 is strongly induced by bacterial stimuli (e.g. LPS) and inflammatory mediators (e.g. TNF- α)[32].

1.4.1   Actions

Defensins are thought to exert a direct antimicrobial effect by binding to bacterial membranes, much like other cationic peptides (e.g. cathelicidin). It is uncertain how they carry out the killing reaction once bound, but permeabilization and pore formation are commonly suggested[28; 31]. However, a single mechanism for the antimicrobial effect of defensins is difficult to justify, as humans possess many different defensin peptides, and structural variation among these would surely affect their mode of action. It has been suggested that the tissue-dependent distribution of different defensins, places them in contact with organisms against which they are most effective[31].

Other activities have also been suggested for defensins. Many defensins are chemoattractants that aid in the recruitment of immune cells to sites of infection. For example, hBD-2 is chemotactic for mast cells, T lymphocytes, and various phagocytic cells. This can enhance the inflammatory response, adaptive immune response, and antimicrobial effect, respectively. In addition, defensins can bind to microbial antigens and deliver them to dendritic cells, leading to induction of adaptive immunity via stimulation of antigen-specific T-cells[28]. These AMPs can also induce TNF-α and interleukin-1 (IL-1) production[28], leading to increased expression of defensin genes (e.g. hBD-2)[32]. Therefore, it is important that some defensins act to control these responses via a negative feedback mechanism[30].

1.5   Vitamin D, AMPs and respiratory tract infection

The presence of vitamin D receptors (VDRs) in most cells of the immune system suggests that vitamin D plays a role in the regulation of immunity[2], both innate and adaptive[12]. Of particular relevance to this study, is the involvement of vitamin D in the expression of human cathelicidin (hCAP-18/LL-37) and β defensin-2 (hBD-2) in the respiratory tract.

The respiratory immune system is extremely important for the protection of the large surface area exposed to inhaled environmental threats, such as microorganisms. In addition to the physical defences provided by cilia and mucus, antimicrobial peptides are thought to play a vital role[33; 34; 35].

The epithelial cells of the lungs and respiratory tract have been shown to produce both LL-37 and hBD-2, and their expression is upregulated in response to microbial invaders[34; 35; 36]. Recognition of these foreign organisms is thought to occur via Toll-like receptors (TLRs), which can then regulate the expression of a variety of genes, including antimicrobial peptides and cytokines[34]. Evidence of AMP induction in response to respiratory infection has been indicated in a number of studies, where peptide levels are significantly higher in patients suffering from, for example, pneumonia[36] or cystic fibrosis (CF), than in healthy controls. One proposed explanation for the frequent infection observed in CF patients is the high salt concentration of the airway surface fluid, which is known to drastically reduce the bactericidal activity of antimicrobial peptides[34; 35].

The enzymes responsible for the conversion of vitamin D to its active form are not only found in the liver and kidneys, but also in various cells of the immune system (e.g. macrophages)[4]. It has been suggested that vitamin D plays a role in the regulation of AMP expression, and that deficiencies can lead to an impaired immune response[33].

Microbial stimulation of TLR-2 induces expression of CYP27B1 – the enzyme responsible for converting the storage form of vitamin D (25D) into the active metabolite (1,25D), and increasing the amount available for binding to the receptor[7; 37; 38]. Once bound to the VDR, vitamin D exerts its biological effects on target genes by binding to response elements (VDREs) in their promoter regions. These elements have been identified in the hCAP-18 gene (CAMP), and it has been shown that 1,25D can increase CAMP expression[39]. Wang *et al.*[40] showed

that VDREs are also present in hBD-2 genes, but noted that induction by 1,25D is much more significant for CAMP. In addition, Liu *et al.*[38] showed that the lower vitamin D levels often found in the serum of individuals with more melanin (e.g. African-Americans) did not allow the same level of TLR-mediated cathelicidin induction as Caucasian serum. However, they also demonstrated that similar levels of induction could be obtained in the African-American subjects after supplementation with vitamin D.

In 1981, Hope-Simpson suggested that the seasonality of influenza was associated with some aspect of solar radiation[33], and since then, many studies have investigated the relationship between low vitamin D levels and increased incidence of respiratory infection. For example, Muhe *et al.*[14] found a strong correlation between cases of rickets and pneumonia in Ethiopian children, and Laaksi *et al.*[41] found that Finnish military recruits with lower vitamin D levels had more frequent absenteeism due to respiratory infection.

As AMP expression is involved in protecting against respiratory infection, and appears to be influenced by vitamin D, it seems logical to infer that individuals with low vitamin D levels will also have low AMP expression and, as a result of this impaired immune response, would be expected to suffer from more severe infections. A recent study on haemodialysis patients used this logic to investigate the relationship between vitamin D, hCAP-18 and mortality due to infection. The results showed that while hCAP-18 levels were strongly associated with mortality, their correlation with vitamin D was not statistically significant[39].

This study will focus on the relationship between AMPs and vitamin D in community acquired pneumonia (CAP) and exacerbations of chronic obstructive pulmonary disease (COPD) – respiratory conditions thought to involve microbial infection. Although smoking is a known risk factor for COPD, a full understanding of the basis of the disease is not yet known[12]. Exacerbations of this condition may be caused by bacterial infection, or by viral infections (particularly rhinovirus) – which have been implicated in up to a third of cases[42]. This study may help identify whether vitamin D has potential as a therapeutic agent for the reduction of infection and inflammation in these conditions[12].

1.6   Vitamin D binding protein

Vitamin D binding protein (DBP) was initially identified as group-specific component (Gc-globulin), and is found in plasma at concentrations of 300-600 μg/mL[43]. It belongs to the albumin superfamily of genes, which forms a cluster on chromosome 4, and also contains albumin, afamin and α-fetoprotein. The 51–59 kDa polypeptide is made up of 458 amino acids, and has two binding regions, which are responsible for its two main biological functions. The first of these is the vitamin D binding domain, where vitamin D and its metabolites are bound for transport throughout the circulation[43; 44; 45]. DBP-bound metabolites have a longer half-life than the free forms, meaning the binding protein can delay the removal of the vitamin from the body, and thereby increase its period of activity[43].

There is a large excess of DBP in comparison to ligand however, and it has been suggested that this is required for the other major role of DBP – actin scavenging via the actin binding domian[43]. Cell death triggers the release of globular actin (G-actin) into the circulation, where it can polymerise to form filamentous actin (F-actin). These filaments can obstruct blood flow and cause organ failure. To prevent this, the gelsolin protein breaks F-actin into G-actin, which is then sequestered by DBP[43; 44; 45].

Several other roles of DBP have also been suggested, including acting as a co-chemotactic factor, and a macrophage-activating factor (MAF)[43; 44; 45].

1.6.1   Polymorphisms

The DBP is highly polymorphic, with three common alleles (Gc-1F, Gc-1S and Gc-2) and more than 120 rare alleles[43; 45]. Some of these rare polymorphisms may reach higher levels in specific populations (e.g. Australian Aborigine and Chippewa Indians have a number of variants that are rare in Caucasian populations)[46]. The three common alleles arise as a result of single nucleotide polymorphisms (SNPs) which cause single amino acid substitutions (Table 1.1)[44]. This gives rise to six common DBP phenotypes: Gc1F-1F, Gc1F-1S, Gc1F-2, Gc1S-1S, Gc1S-2, and Gc2-2[45].

Table 1.1 – Amino acid residues that produce Gc-globulin isoforms, modified from Christiansen *et al.*[44]

Isoform	Amino acid residue at position 416	Amino acid residue at position 420	Theoretical molecular weight (Da)
Gc-1F	D	T	51188
Gc-1S	E	T	51202
Gc-2	D	K	51215

The frequency of each allele varies with geographical region[43; 46], and it has been suggested that there is a correlation between allele frequency and degree of skin pigmentation. For example, Gc-1F has a higher efficiency of vitamin D transport, and binds it with more affinity, and the frequency of this variant is highest in dark-skinned populations (where UV-mediated vitamin D synthesis is lower)[43].

Fu *et al.*[47] demonstrated that mean vitamin D (25D) levels vary with genotype at position 420 (T436K SNP), with lowest levels present in K allele homozygotes (KK). They also showed that individuals respond differently to vitamin D supplementation, depending on their DBP genotype. In this case, KK homozygotes showed the most significant increase in plasma concentration after supplementation, followed by TK, and finally TT individuals. On the other hand, the presence of D versus E alleles at position 416 (D432E SNP) did not show a significant correlation with baseline 25D or supplementation effect.

1.6.2   DBP and COPD

Many studies have focussed on the clinical significance of the DBP isoforms[43; 45], and some have found a relationship between genotype and risk of developing chronic obstructive pulmonary disease (COPD)[43; 48; 49; 50].

Airway inflammation and obstruction of airflow are the main characteristics of this respiratory disease, the chief risk factor for which is cigarette smoking. However, the observation that the majority of smokers do not develop COPD[48; 50], and that it shows familial associations, led to the suggestion that there was a genetic component to the disease[49; 50].

A number of groups have investigated the relationship between the three common DBP polymorphisms, and risk of COPD development. Both Ishii et al.[48] and Ito et al.[49] showed that the frequency of the Gc-1F allele was higher in COPD patients than in healthy controls, and that homozygous 1F-1F genotypes appear to increase the risk of disease development further. It is important to note however, that the frequencies of these alleles vary with different populations, and both studies were carried out using Japanese subjects. Schellenberg et al.[50] could not confirm this finding in a study using Caucasian participants, but attributed this to the low frequency of the Gc-1F allele in this population giving an insufficient number of individuals for significance. However, this group did find that the frequency of the homozygous Gc2-2 genotype was significantly lower in the COPD group than the controls, suggesting it may have a protective effect. The same could not be said for the heterozygotes, however.

Although the reason behind these differences in COPD risk between DBP variants has not yet been determined, it is thought to be associated with the role of DBP as a macrophage-activating factor (MAF). For conversion to MAF, DBP undergoes deglycosylation. The sugar side chains that are removed in this process are the same in Gc-1F and Gc-1S, but absent in Gc-2. This means that Gc-2 cannot be converted, and less MAF is produced in individuals with that genotype. This means that these individuals may have a reduced inflammatory response, and therefore less lung damage[49; 50].

2. Experimental

Note – See Appendix 6.1 for buffer and solution recipes, grouped by method.

2.1   Determination of vitamin D status and infection severity

This study gained approval from the Northern Y (NTY/08/05/045) and University of Waikato Human Research (Protocol #93) ethics committees.

Members of the Department of Respiratory Medicine at Waikato Hospital carried out the measurements of vitamin D status and infection severity. Patients admitted to the department with community acquired pneumonia (CAP) or acute exacerbations of chronic obstructive pulmonary disease (COPD) were invited to participate in the study, and written consent was obtained from those who accepted.

Blood samples were taken from these patients within 24 hours of admission, and the concentration of vitamin D determined by competitive electrochemiluminescence immunoassay (Elecsys, Roche Diagnostics). Measures of co-morbidities and infection severity were also performed, using the Charlson Index score and the CURB65 score, respectively[51].

2.2   ELISA

2.2.1   Quantification of β defensin-2 in human plasma

The plasma concentration of human β defensin-2 (hBD-2) in each sample was determined using the Human BD-2 ELISA Development Kit (PeproTech Inc, 900-K172), according to the instructions of the manufacturer.

Reconstituted capture antibody was diluted 1:400 in phosphate buffered saline (PBS) to a concentration of 0.25 µg/mL, and 100 µL was added to each well of a 96-well plate. The plate was covered in foil and incubated overnight at room temperature, then washed four times using 200 µL of wash buffer (0.05% Tween-20 in PBS) per well. Block buffer (1% BSA in PBS) was added at 200 µL per well, and the was plate incubated at room temperature for at least 1 h, before being washed in PBS-Tween, as above. Human BD-2 standard was serially diluted with diluent (0.05% Tween-20, 0.1% BSA in PBS) to give standard concentrations of 1000, 100, 10 and 1 pg/mL, and 100 µL of each was added to the plate in duplicate. A blank (diluent only) and the plasma samples were also

added in duplicate, at 100 µL per well. The plate was incubated overnight at 4 °C, and washed four times. Reconstituted detection antibody was diluted 1:200 (in diluent) to 0.5 µg/mL, and 100µL added to each well. After incubating at room temperature for 2 h, and washing the wells four times, 100 µL of avidin-HRP conjugate (diluted 1:2000 in diluent) was added per well. The plate was washed again before adding 100 µL of ABTS (2,2'-Azino-Bis(3-Ethlybenzthiazoline-6-Sulfonic Acid); Sigma, A 3219) substrate to each well. Colour development was monitored at 5 min intervals for 30 min using an ELISA plate reader (FLUOStar Optima) at 405 nm, with a wavelength correction of 690 nm. A standard curve was generated to allow determination of sample concentrations of hBD-2 (see Appendix 6.3 for an example calculation).

2.2.2   Quantification of LL-37 in human plasma

The LL-37 concentration in each plasma sample was determined using the Human LL-37 ELISA Test Kit (Hycult Biotechnology, HK321), according to the instructions of the manufacturer.

Briefly, reagents were reconstituted as instructed, and samples brought to room temperature. The LL-37 standard was serially diluted in wash/dilution buffer to give a concentration range of 100, 22.3, 11.1, 3.7, 1.2, 0.4 and 0.1 ng/mL. A blank of 0 ng/mL was also prepared as a control. The blank and standards were added to the plate in duplicate, at 100 µL per well, as were the plasma samples (diluted 1:20 in wash/dilution buffer). The plate was incubated at room temperature for 1 h, and washed four times with 200 µL of wash/dilution buffer per well. Tracer was added at 100 µL per well, and incubated for 1 h at room temperature. After washing as above, 100 µL of streptavidin-peroxidase conjugate was added to each well, incubated for 1 h at room temperature and washed four times. TMB (tetramethylbenzidine) substrate was added (100 µL per well) and the plate incubated for 20-30 min in the dark. The reaction was stopped by adding 100 µL of stop solution per well, and the absorbance was measured at 450 nm using a plate reader (FLUOStar Optima).

2.3   Purification of plasma peptides

2.3.1   Albumin removal and TCA precipitation

The plasma purification protocols of Colantonio et al.[52] and Jiang et al.[53] were combined to improve detection of small peptides, as suggested by McKenzie[54].

To each plasma sample, 1 M sodium chloride (NaCl) was added to give a final concentration of 0.1 M, and the samples were incubated at 4 °C on a rotating mixer for 1 h. Cold ethanol was added to give a final concentration of 42%, and the samples were centrifuged for 45 min at 13,000 rpm and 4 °C. The pellet (pellet 1) was retained, and the pH of the supernatant lowered to 5.7 with 0.8 M sodium acetate (NaAc). The supernatants were incubated at 4 °C for 1 h, and centrifuged for 45 min at a speed of 16,000 g, to produce pellet 2.

Pellets 1 and 2 of each sample were combined and resuspended in 200 μL of PBS and 40 μL of 60% trichloroacetic acid (TCA). The samples were incubated overnight at -20 °C, and centrifuged for 30 min at 10,000 g and 4 °C. The supernatant was discarded and 300 μL of cold acetone added to wash each pellet. The samples were incubated on ice for 15 min, and centrifuged as above. Finally, the acetone was removed, and the pellet left to air dry.

To run the samples on a gel, pellets were resuspended in water and gel loading buffer (GLB), heated to 95 °C for 5 min, and briefly centrifuged so the supernatant could be loaded.

2.3.2   TCA precipitation

To perform the TCA precipitation step only, PBS was added directly to 12.3 μL of plasma to give a final volume of 200 μL, before proceeding to the TCA step, as described above.

2.3.3   Acetic acid and methanol precipitation

Cole and Ganz [55] suggest the use of acetic acid and methanol to precipitate out unwanted material, but leave antimicrobial peptides in the supernatant fraction. A method employed by Tang et al.[56] to isolate α-defensins from leukocytes also used this idea, so was tested to determine whether it was as effective in the purification of other antimicrobial peptides from plasma.

To 100 μL of plasma, 900 μL of 80:10 methanol:acetic acid was added and stirred for 18 h, then centrifuged. Supernatants were dried in a SpeedVac and resuspended in 1 mL of 80:20 methanol:water. Samples were stirred for 6 h, centrifuged and dried as above, and acidified by adding 0.1 mL 5% acetic acid. The supernatant obtained after a final centrifugation step was retained and mixed with gel loading buffer for electrophoresis.

2.3.4   C-18 Filter Tips

Eppendorf PerfectPure C-18 pipette tips were also used in some cases, to further process the supernatant before analysis. These tips act to desalt the sample, and have a pore size that makes them selective for peptides with molecular weights of less than 15 kDa. The tips were applied to a pipette set at 10 μL, and pre-wet solution (50% acetonitrile (ACN), 0.1% trifluoroacetic acid (TFA)) was taken up and discarded several times, without allowing air to enter. This was repeated using equilibration/wash solution (0.1% TFA), before aspirating and expelling the sample up to ten times, followed by equilibration/wash solution up to five times. Elution solution (75% ACN, 0.1% TFA) was aspirated at least three times, before dispensing into a clean tube. This eluate was either mixed with gel loading buffer for electrophoresis, or with matrix on a target for mass spectrometry (MS).

2.4   Gel Electrophoresis

2.4.1   Tris-Tricine SDS-PAGE

Tris-Tricine gels are used in cases where the separation of small proteins (<30 kDa) is required. These gels were prepared according to the method described by Schägger[57] (Table 2.1), using a solution of acrylamide:N,N'-methylenebisacrylamide at a concentration of 49.5%, with 3% or 6% cross-linking (AB-3 or AB-6, respectively). Using higher percentage gels with a greater degree of cross-linking is suggested to improve the separation of small peptides. Other suggestions include the addition of urea or the use of spacer gels between the stacking and separating layers[57].

Table 2.1 – Recipe for large Tris-Tricine gel

STOCK SOLUTION	Stacking Gel	Separating Gel			
	4%	10%	12.5%	16%	16%/6 M urea
AB-3 or AB-6 (mL)	1	6	7.6	10	10
3x Gel Buffer (mL)	3	10	10	10	10
Glycerol (g)	-	3	3	3	-
Urea (g)	-	-	-	-	10.8
Add water to final volume (mL)	12	30	30	30	30
10% (w/v) APS (µL)	90	150	150	100	100
TEMED (µL)	9	15	15	10	10

To prepare each gel, the glass plates were cleaned with ethanol and acetone, and assembled. The desired gel concentration was determined, and the corresponding volumes of AB-3 (or AB-6), gel buffer, water, and glycerol were added to a flask. To prevent polymerization occurring too early, tetramethylethylenediamine (TEMED) and 10% (w/v) ammonium persulphate (APS) were added last. Immediately after APS addition, the solution was mixed, taken up in a syringe, and poured between the assembled plates. A layer of 2-butanol was added to level the top of the gel, and prevent it from drying out. Once the separating gel had set, the butanol was removed and the stacking gel prepared and applied on top. The gel comb was carefully inserted into this layer, which was then left to polymerize.

To run the gel, the plates were secured to the electrophoresis apparatus, and cathode and anode buffer were placed in the upper and lower buffer chambers respectively. The gel was pre-electrophoresed at 18 mA for 15 min, before loading the samples, standards, and molecular weight ladder (Bio-Rad Polypeptide SDS-PAGE Molecular Weight Standards, 161-0326).

The current was maintained at this level until the gel front progressed past the stacker and into the separating gel, at which point it was increased to about 45 mA, until the gel front reached the bottom.

2.4.2   Laemmli SDS-PAGE

Laemmli gels are more suitable for larger proteins (>30 kDa)[57], and the size of the protein of interest will determine the separating gel percentage to be used. Basically, separation of smaller proteins requires a more concentrated gel.

The gels were prepared using the method described by Coligan *et al.*[58] (Table 2.2), and concentrations of 7-12% were used.

Table 2.2 – Recipe for large Laemmli Gel

STOCK SOLUTION	*Stacking Gel*	Separating Gel			
		7%	7.5%	10%	12%
30% acrylamide/0.8% bis (mL)	0.65	3.50	3.75	5.00	6.00
4 x Tris-Cl/SDS pH 8.8 (mL)	-	3.75	3.75	3.75	3.75
4x Tris-Cl/SDS pH 6.8 (mL)	1.25	-	-	-	-
Water (mL)	3.05	7.75	7.50	6.25	5.25
10 % (w/v) APS (µL)	25	50	50	50	50
TEMED (µL)	5	10	10	10	10

The same assembly and electrophoresis conditions used for Tris-Tricine gels were employed. However, for the Laemmli gels, both buffer chambers were filled with 1x SDS electrophoresis buffer, and a different molecular weight ladder (Bio-Rad Precision Plus Protein Standards (Dual Colour), 161-0374) was used.

2.5   Gel Staining

2.5.1   Blue-Silver

Gels were fixed in 50% methanol, 2% phosphoric acid for 30-40 min, stained overnight in blue micellar solution, and destained in 5% methanol. Bands of interest were excised from the gel for further analysis (see section 2.6).

2.5.2   Silver

i.   Basic Silver Staining

Gels were fixed for 15 min in 100 mL fixing solution, and washed in 100 mL 30% ethanol for 2 min. Gels were then sensitized by soaking in 100 mL 0.02% sodium thiosulfate for 1 min. Excess sensitizer was removed by washing gels twice in Milli-Q water (10 seconds each), before staining for 10 min. After repeating the Milli-Q washes, gels were soaked in developer until bands appeared. Once visible, the reaction was stopped by removing the developer and adding 100 mL of 10% acetic acid.

Note: When silver staining a gel that had already been stained with blue-silver, excess Coomassie was removed by washing in Milli-Q, then gels were taken straight to the sensitizing step of the basic silver staining protocol (i.e. 1 min in 0.02% sodium thiosulfate).

ii.   Alternative Silver Staining Protocols

The basic silver staining method is not compatible with matrix-assisted laser desorption/ionization time-of-flight (MALDI-TOF) mass spectrometry. For this reason, the alternate protocols used by He et al.[59] and Yan et al.[60] were trialled in an attempt to improve detection of small, low abundance peptides, while mainitaining MS-compatibility.

a)   He Silver Staining

Gels were fixed overnight in a 30% ethanol, 10% acetic acid solution, and soaked in sensitizer for 30 min. After three 5 min water washes, gels were stained for 40 min, and incubated in developer for 15 min. This reaction was stopped by adding 1.46 % EDTA, followed by three 5 min water washes.

b)   Yan Silver Staining

Gels were incubated twice in fixing solution, for 15 min per wash, and sensitized for 30 min. After three 5 min washes in Milli-Q, gels were stained for 20 min, and washed another two times in water for 1 min each. Bands were visualised by incubating in developer, before stopping the reaction by washing with 1.46% EDTA for 10 min.

2.6   In-gel digestion (for Blue-Silver stained gels)

Bands of interest in blue-silver stained gels were either cut out using a scalpel, or extracted as a plug using a glass pipette. Excised bands were destained overnight in 1:1 acetonitrile:25 mM ammonium carbonate, and then washed for 15 min in the same solution, followed by 15 min in ACN. After removal of this solution, the gel plugs were dried (air or SpeedVac), and 10 µL of Promega Trypsin Gold (diluted 1:200 in 25 mM ammonium carbonate) was added. The samples were incubated at 4 °C for 1 h to allow the trypsin solution to rehydrate the gel pieces. Excess trypsin was removed and samples were incubated at 37 °C for 4-6 h. To prevent evaporation during this time, parafilm was wrapped around the top of each tube. Finally, samples were incubated overnight at 4 °C in 10 µL of 20% ACN, 0.1% TFA. This solution acted to aid diffusion of proteins out of the gel pieces, and helps ionize the peptides for mass spectrometric analysis.

2.7   MALDI-TOF mass spectrometry

All mass spectrometry was performed on an Autoflex[TM] II MALDI-TOF mass spectrometer (Bruker Daltonics) using FlexControl[TM] software, and spectra were analysed using FlexAnalysis[TM] and BioTools (Bruker Daltonics).

2.7.1   Sample Preparation and loading
i.   Dried Droplet

For a dried droplet preparation, 0.5 µL of matrix was added to the target plate followed by an equal volume of sample. The two were pipetted up and down several times to mix, then left to dry.

Dried droplet can be used on AnchorChip, aluminium or steel targets, but the latter two allow the sample to be dispersed over a larger area, which may be better for detection.

ii.   Thin Layer

A saturated solution of α-Cyano-4-hydroxycinnamic acid (CHCA) matrix in acetone was prepared and 10 μL dragged across the target. The acetone evaporated, leaving a thin layer of matrix on the hydrophilic centres of the AnchorChip target plate. To each of these centres, 0.5 μL sample was applied and left to dry.

iii.   Washing

A washing step can be included in both dried droplet and thin layer methods. The wash solution used was a 9:1 mixture of 0.1% trifluoroacetic acid (TFA):100 mM ammonium phosphate ($NH_4H_2PO_4$). This is a volatile solution so evaporates off in the vacuum, while acting as a buffer to remove some of the salt and thereby give a better signal. However, washing can also remove some of the sample, particularly in dried droplet preparations.

To perform a wash, 5 μL of the solution was applied to each spot of sample and matrix, and then removed after approximately 5 seconds.

2.7.2   Calibration

A peptide calibration standard (Bruker Daltonics) was mixed with matrix and applied to the MALDI target plate in the same area as the sample spots. Spectra collected from these standard spots were used to calibrate the instrument, before analysing the samples.

2.7.3   Lysozyme Gels

A range of concentrations of lysozyme were run on small 16% Tris-Tricine gels, to determine the cut-off concentration for detection by blue-silver staining. The bands at the lowest detectable concentration were cut out of the gel as whole bands or single plugs, and a comparison of the dried droplet, thin layer,

and washing procedures was carried out. To allow optimum performance of each technique, the dried droplet preparation was performed on a steel MALDI target, and a 600 μm AnchorChip target was used for thin layer.

2.7.4   Plasma Screening

Pellets from the albumin removal/TCA precipitation method were resuspended in 40 μL Milli-Q water, and centrifuged. The supernatants were either applied directly to the MALDI target plate, or were filtered with C-18 tips before loading. The samples were mixed 1:1 with matrix (5 μL each) on an aluminium target, using the dried droplet method. The matrix used was 2,5-dihydroxybenzoic acid with 10% 5-methoxysalicylic acid (super DHB (sDHB)), which had been made up in 40 μL 1:2 ACN:0.1% TFA, to give a saturated solution.

Human beta defensin-2 (hBD2) and cathelicidin (LL-37) standards from their respective ELISA kits were also filtered with C-18 tips, and mixed 1:1 with sDHB matrix on the target.

Sample and standard spectra were collected using a linear detector and high laser power method.

2.7.5   Peptide Fingerprinting

To perform MALDI-TOF on samples excised from gels and trypsin-digested, α-Cyano-4-hydroxycinnamic acid (CHCA) matrix was used. This is a better matrix for the analysis of small peptides because it requires less energy to ionise. A saturated solution of CHCA was made up in 40 μL 2:1 ACN:0.1% TFA, before mixing 1:1 (0.5 μL each) with samples on the target. In most cases, the target used was a 600 μm AnchorChip plate, as this allowed for tandem mass spectrometry.

Analysis of peptide digests was carried out using the reflector detection method. This adjusts for the energy spread of ions, and gives a more resolved peak, which is important for peptide identification. To perform a database search, the Mascot program from Matrix science was used, with the following search parameters: Chordata, trypsin digestion, up to one missed cleavage, a mass tolerance of no more than 200 ppm, and monoisotopic. The National Center for Biotechnology Information nonredundant (NCBInr) database was used, and

protein scores of >73 (as calculated by Mascot) were classed as being significant database hits (p<0.05).

2.7.6   Tandem Mass Spectrometry

Tandem mass spectrometry, using the LIFT[TM] method, enables the analysis of the amino acid sequence of a particular peak of interest from an MS spectrum. The parent ion is fragmented further to (ideally) give single amino acid-length fragments, the spectrum of which can help to ascertain the sequence of that parent ion. This may help in the determination of the identity and possibly even the sequence of the peptide.

2.8   Identification of DBP polymorphisms

2.8.1   Extraction of DNA from Saline Mouthwash

After gaining approval from the University of Waikato Human Research ethics committee (Protocol #95), volunteers were asked to carry out a 0.9% saline mouthwash and dispel the liquid into a 50 mL tube. These were centrifuged at 2,500 rpm for 15 min and the supernatant discarded. To each pellet, 350 μL lysis solution was added and mixed, then transferred to a 1.7 mL eppendorf tube. The samples were heated (while shaking) at 55 °C, for 10 min. An equal volume of 5 M lithium chloride (to salt out the protein), and 750 μL of chloroform were added, and the tubes shaken and placed on a rotating mixer for 30 min. After centrifuging for 10 min, the top layer was transferred to a new tube, and the rest discarded. The DNA was precipitated with an equal volume of isopropyl alcohol for 30-60 min, and centrifuged for 20 min. The liquid was tipped off, and the DNA pellet washed with 1 mL 70% ethanol. After removal of the ethanol, pellets were resuspended in 50 μL TE buffer.

2.8.2   Polymerase Chain Reaction (PCR)

Polymerase Chain Reaction (PCR) was performed on the extracted DNA samples to amplify the vitamin D binding protein (DBP) gene, and determine the polymorphisms present. This was carried out using the primers and PCR conditions of Fu *et al.*[47] A 50 μL reaction was prepared for each sample. This included master mix, i-StarTaq[TM] polymerase, and three primers – 0.5 μM of

common forward, 0.5 μM of wild-type reverse, and 0.2 μM of mutant reverse (see Appendix 6.2 for sequences). Excluding the negative control, 2.5 μL DNA was added to each tube. The PCR conditions were set at 95 °C for 2 min, followed by 35 cycles of 95 °C for 20 sec, 58 °C for 20 sec, and 72 °C for 20 sec. At the end of the last cycle, an additional step of 68 °C for 5 min was included.

The PCR products were run on 2% agarose/1xTAE gels containing ethidium bromide, with 6x loading buffer and 1x TAE running buffer. The Invitrogen 100 bp ladder was used for all gels to allow the approximate size of bands to be determined when visualised under UV light.

2.8.3   Restriction Enzyme Digestion

To determine the D432E genotype, 10 μL of the PCR amplified mixture was incubated overnight at 37 °C, with 1 μL of the restriction enzyme HaeIII. The restriction enzyme digests were then run on 2% agarose/1x TAE gels, as above.

2.8.4   Touchdown Protocol

A different PCR protocol was also trialled, with conditions: 95 °C for 2 min; 10 cycles of 20 sec at 95 °C and 20 sec at 62.5 °C (-0.5 °C per cycle); 35 cycles of 20 sec at 95 °C, 20 sec at 58 °C and 72 °C for 20 sec; and finally 68 °C for 5 min. In this case, mutant and wild type reverse primers were run as separate reactions.

2.8.5   Purification of PCR products for sequencing (PEG precipitation)

Polymerase chain reaction (PCR)-amplified products were pipetted into 1.7 mL Eppendorf tubes, and an equal volume of polyethylene glycol (PEG) was added. After leaving to precipitate for at least 10 min, the mixture was centrifuged and the liquid poured off. The pellet was washed by adding 1 mL 100% ethanol and centrifuging for 5 min, before tipping off the liquid and repeating with 70% ethanol. After removing all the liquid, 10 μL Milli-Q water was added, and the tube vortexed to resuspend the pellet. The DNA concentration was measured by NanoDrop, and submitted for sequencing along with the common forward primer, at a concentration of 5 pmol/μL.

3.   Results and Discussion

3.1   Determination of vitamin D status and infection severity

Vitamin D deficiency is defined as a serum concentration of less than 50 nmol/L, and 49% of all the study patients fell within this category. Of these, 35% (i.e. 17% of all patients) were severely deficient, with levels of <30 nmol/L.

The CURB65 score takes into account a number of clinical factors (e.g. blood pressure, respiration rate), and uses them to assign a number (between 0 and 5) to patients with pneumonia or exacerbations of COPD. This number predicts the risk of 30-day mortality, and therefore acts as a marker for infection severity, with lower scores representing milder infections and reduced chance of death.

Table 3.1 shows the vitamin D and CURB65 score statistics for all the study patients, and for the CAP and COPD groups individually. The average CURB65 score overall was 2, and was higher among patients who died within 30 days (average = 3) than those who did not (average = 2).

Table 3.1 – Vitamin D status, CURB65 and 30-day mortality statistics of patients with respiratory tract infection

	All patients n = 185	CAP patients n = 112	COPD patients n = 73
Vitamin D status			
Severely deficient (<30 nmol/L)	17.30%	15.18%	20.55%
Deficient (30-49 nmol/L)	31.89%	28.57%	36.99%
Sufficient (≥50 nmol/L)	50.81%	56.25%	42.47%
CURB65 score			
0-1	30.27%	28.57%	32.88%
2-3	55.14%	52.68%	58.90%
4-5	14.59%	18.75%	8.22%
30-day mortality Number of patient deaths within 30 days	9.73%	8.04%	12.33%

As shown in Figure 3.1, an assessment of the average vitamin D concentration at each CURB65 score did not reveal any significant trend, but it did highlight the fact that patients with COPD had lower average vitamin D levels across all scores, and no COPD patients reached the highest risk level (CURB65 score of 5).
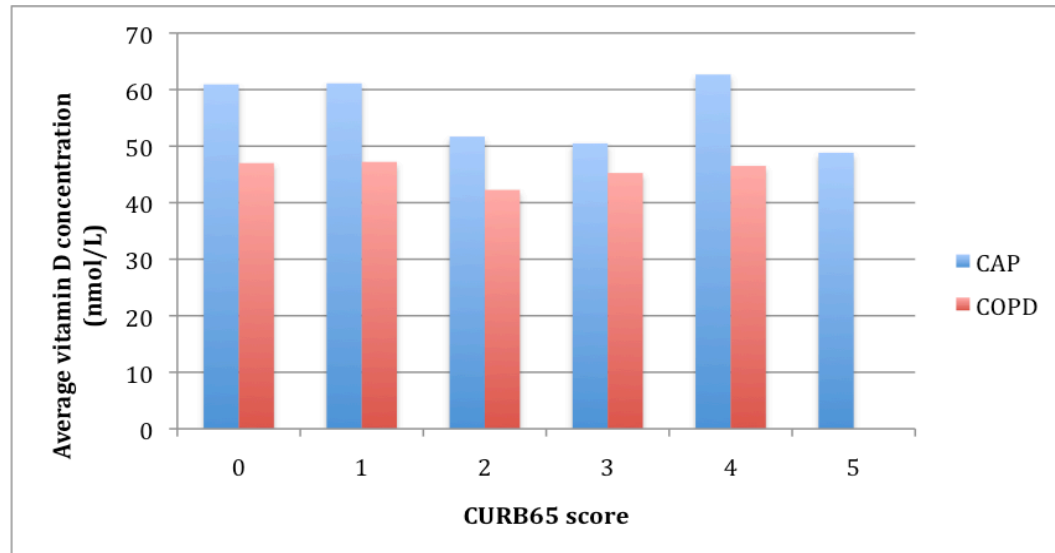
Figure 3.1 – Comparison of average vitamin D concentration and CURB65

However, a comparison of vitamin D status and mortality did reveal a relationship. Whether pneumonia and COPD were analysed individually or together, mortality was substantially higher in patients with severe deficiency. In addition, data collected from pneumonia patients follows a clear trend, with highest mortality rates in patients with severe deficiency (29.41%), followed by those with a mild deficiency (6.25%), and lowest rates in those with adequate levels of vitamin D (3.17%), as shown in Figure 3.2. This trend can also be seen when assessing the two respiratory infections together, but not when analysing COPD data alone, as patients with adequate amounts of vitamin D had higher rates of mortality (12.90%) than those classed as mildly deficient (7.41%).

Together, these results indicate that the serum 25D concentration is not directly related to CURB65 in pneumonia or exacerbations of COPD, nor is it predictive of mortality in COPD. These conclusions were confirmed after log-transformation of the data and logistic regression analysis, which showed that the CURB65 score is a predictor of mortality (p=0.001), while 25D (grouped according to status) is significant in pneumonia (p=0.002), but not in COPD (p=0.489).
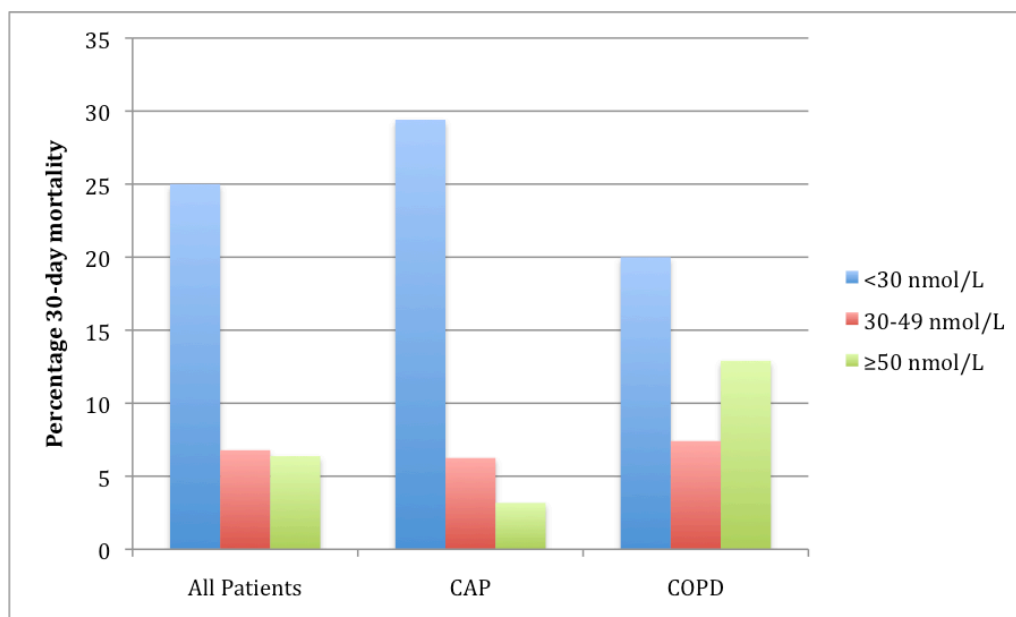
Figure 3.2 – Relationship between 30-day mortality and vitamin D status

3.2   Plasma hBD-2 and LL-37 levels by ELISA

Indirect ELISA was used to determine the concentrations of LL-37 and hBD-2 in the plasma of patients with pneumonia and acute exacerbations of COPD (see Appendix 6.3 for full results). The mean and median were higher in pneumonia for both antimicrobial peptides, but COPD patients exhibited a wider concentration range (Table 3.2).

Table 3.2 – Basic statistics for LL-37 and hBD-2 as determined by ELISA

	LL-37 concentration (ng/mL)		hBD-2 concentration (pg/mL)	
	CAP	**COPD**	**CAP**	**COPD**
Mean	80.41	65.58	421.37	342.87
Median	68.46	59.99	261.55	188.38
Range	13.16 - 263.49	10.26 - 341.25	13.96 - 1733.62	15.31 - 2469.39

These ELISA results were divided into tertiles and compared to 30-day mortality, to determine whether any correlation existed (Figure 3.3 a-c).
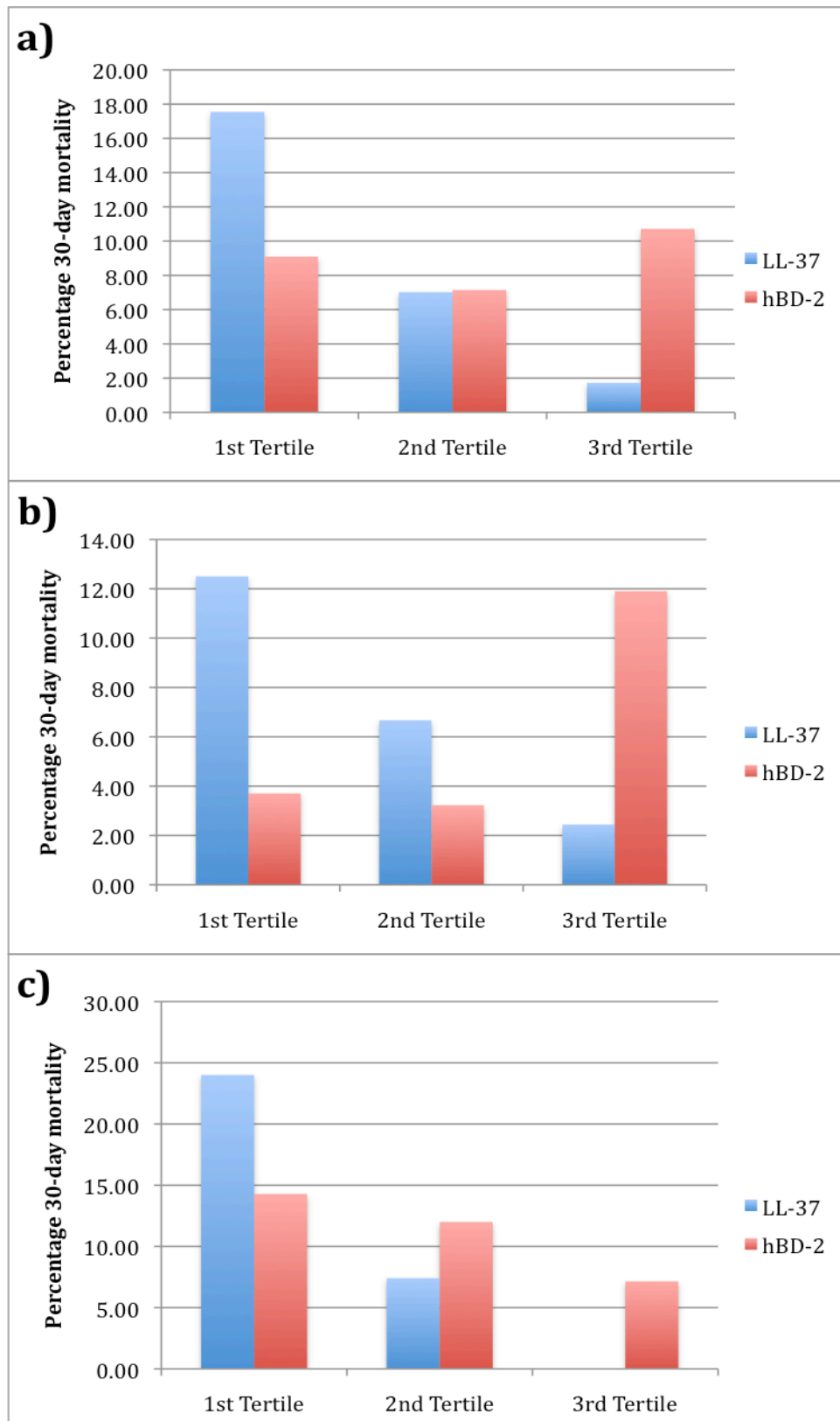
Figure 3.3 – Relationship between percentage 30-day mortality and concentration of LL-37 and hBD-2 in a) Both CAP and COPD, b) CAP only, and c) COPD only

3.3   Discussion of relationships between hBD-2, LL-37, vitamin D and 30-day mortality

The presence of vitamin D response elements (VDREs) in the promoter regions of both LL-37 and hBD-2 genes led to the hypothesis that patients with low levels of vitamin D would have correspondingly low concentrations of these antimicrobial peptides. Spearman's non-parametric correlations were used to determine whether any relationships existed between these variables, as all three showed skewed distributions.

No significant correlations where found between 25D and LL-37 (p=0.549), 25D and hBD-2 (p=0.990), or LL-37 and hBD-2 (p=0.405), and this lack of significance remained when analysing pneumonia and COPD individually.

Therefore, although previous studies have shown the ability of 1,25D to induce both LL-37 and hBD-2, the present findings do not support the hypothesis of a direct relationship between vitamin D status and antimicrobial peptide level, and indicates that other factors must influence the expression levels of these VDRE-containing genes.

Any factor involved in the uptake of 25D into target cells, the conversion of 25D to 1,25D, the levels of VDR, or the formation and binding of the VDR-RXR complex to VDREs, could conceivably affect the expression of such target genes. For example, as the binding of 1,25D to the receptor is the first step in the vitamin D-mediated gene expression pathway, VDR upregulation (e.g. by 1,25D or protein kinase A) or downregulation (e.g. by protein kinase C) would influence the capacity for regulation of downstream targets. In addition, transcription factors (TFs) or coregulatory elements such as NF-κB are required to bind to the VDR-RXR complexes at VDRE sites, in order for the target genes to be expressed. Therefore, the availability of these elements could also influence the levels of vitamin D-regulated gene products[61].

Another possibility for the lack of association between antimicrobial peptide concentration and vitamin D status may be that the serum 25D level is used to determine the status, while 1,25D is the active form that interacts with the VDR to mediate changes in gene expression. Therefore, a relationship may exist between 1,25D and these AMPs that is not seen when using standard clinical measures.

Further statistical analyses were carried out after log transformation of the data. This made the data assume a more normal distribution, and thereby allowed parametric tests to be used.

As discussed in section 3.1, the relationship between plasma 25D status and 30-day mortality was significant only in pneumonia. Using the data from both respiratory infections together, the relationship between 25D and 30-day mortality reaches a higher significance (p=0.001 compared to 0.006) if vitamin D is analysed as low (<30 nmol/L) or not (≥30 nmol/L), rather than as a continuous variable (i.e. by status – severely deficient, deficient, or sufficient). In addition, logistic regression showed that the relationship between 30-day mortality and low vitamin D remained after adjusting for sex, age, and diagnosis (pneumonia or COPD). Based on these findings, "low vitamin D" was used as the 25D variable in further analyses.

Figure 3.3 (a-c) suggests that lower plasma LL-37 concentrations are associated with a higher risk of 30-day mortality, whether analysing pneumonia and COPD together, or individually. Logistic regression confirmed this finding, and showed that plasma LL-37 remains a strong predictor of 30-day mortality after adjusting for age, sex, diagnosis, CURB65 score, Charlson index, hBD-2 level, and low vitamin D. Individual analysis however, showed that the relationship between LL-37 and 30-day mortality was not significant in pneumonia patients (p=0.251).

These findings for LL-37 are consistent with those of Gombart *et al.*[39] who showed that the cathelicidin precursor, hCAP-18, was strongly associated with mortality in patients undergoing haemodialysis, but did not have a statistically significant relationship with vitamin D. In addition, thirty patients in the present study used supplements to boost their vitamin D intake. Comparison of these patients with those not taking additional vitamin D showed that while 25D levels were significantly increased in the supplemented group (p=0.0001), LL-37 was not (p=0.835).

No association was found between hBD-2 and 30-day mortality in pneumonia (p=0.262) or COPD (0.797). This remained the case when assessing the two infections together (0.803), and after adjusting for low vitamin D, cathelicidin level, age, sex, diagnosis, CURB65 and Charlson index.

Lower plasma levels of LL-37 were found to be associated with increased mortality in COPD patients and, despite the lack of statistical significance, showed a similar trend in pneumonia (Figure 3.3 b). This is consistent with the hypothesis that lower antimicrobial peptide levels reduce the effectiveness of the innate immune response, and result in infections with a higher severity. In this case, severity was measured in terms of 30-day mortality, as the relationship between LL-37 and CURB65 was not statistically significant (Figure 3.1). This increased mortality in patients with lower LL-37 levels lends further support to the idea that this antimicrobial peptide is essential to human survival, as is clearly demonstrated in morbus Kostmann patients.

It is possible that hBD-2 levels do not show such a relationship with 30-day mortality because they are not as indispensable as LL-37. This may be due to the fact that humans have several β-defensin genes, but only one for cathelicidin. These different defensins have a certain degree of overlap in their tissue distribution, and therefore may be able to substitute for one another to a certain extent. Alternatively, one of the other defensins may hold a greater importance in these respiratory tract infections than hBD-2, and it may be this peptide that is significantly related to mortality.

3.4   MALDI-TOF as a method for screening plasma LL-37

Although not a quantitative method like ELISA, it was thought that MALDI-TOF mass spectrometry might be able to detect LL-37 in plasma, down to a certain concentration. If so, screening plasma samples to determine which patients had LL-37 levels below this detection threshold, could provide a fast and simple method for identifying those with a higher risk of mortality.

To determine the feasibility of this method, the six plasma samples with the highest LL-37 levels (as determined by ELISA) were screened. Spectra obtained were compared to those generated by MALDI-TOF analysis of the human LL-37 ELISA standard (Figure 3.4). The peaks at approximately 4.56 kDa were in good agreement with that of the standard, and were seen in five of the six plasma samples. Peaks at about 9.2-9.3 kDa were also evident in the standard and at least two samples, and may represent aggregates of cathelicidin molecules. A sample spectrum is shown in Figure 3.5, for comparison.
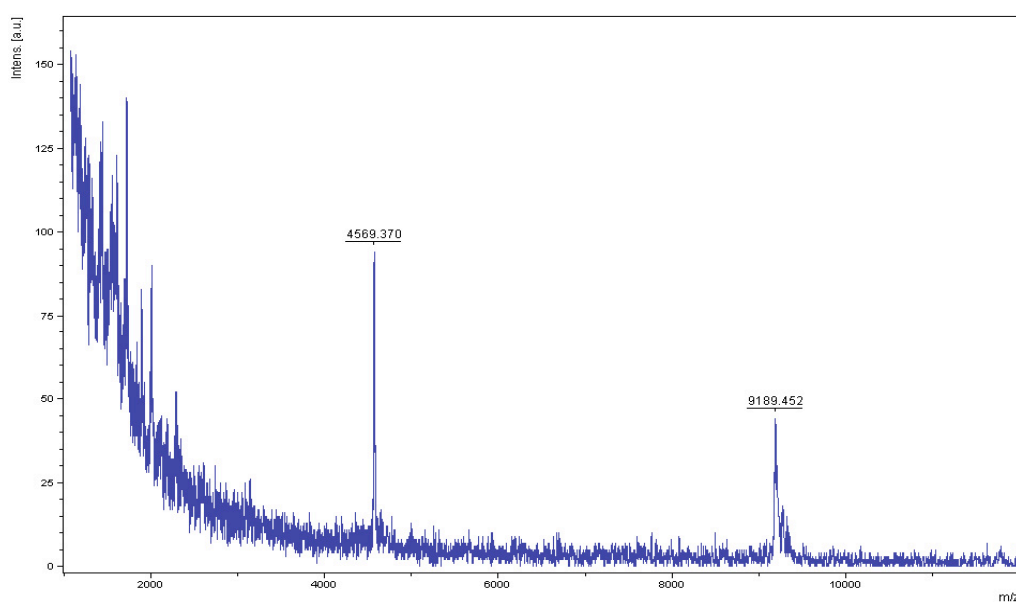
Figure 3.4 – MALDI spectrum of LL-37 standard
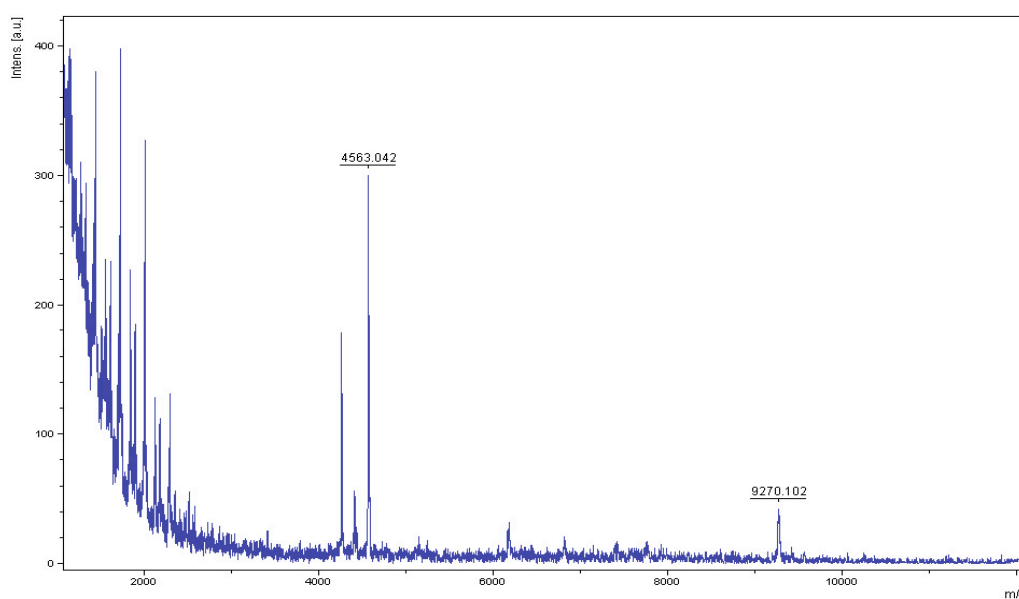
Figure 3.5 – MALDI spectrum of a plasma sample

The hBD-2 standard was also run on the mass spectrometer, and compared to sample spectra to determine if the plasma screens could also detect this antimicrobial peptide. Although some sample peaks did resemble those of the standard, hBD-2 levels in plasma are much lower than those of LL-37 (pg/mL compared to μg/mL), making detection less likely. Therefore, even if a threshold could be obtained, it is likely that it would be at a high concentration, and would therefore not be useful for plasma screens. In any case, hBD-2 levels were not

found to be significantly associated with mortality in either respiratory disease, so the ability to identify patients with lower levels by MALDI-TOF did not have the same clinical potential or importance.

3.5   Tris-Tricine SDS-PAGE detection of LL-37

For the plasma screening method to be used, the identity of the peak at 4.56 kDa needed to be confirmed as LL-37. This required the use of gel electrophoresis, to allow for a more complete purification of LL-37 from other plasma proteins. Bands of interest were excised from the gels and subjected to a tryptic digest, followed by MALDI-TOF. The spectra produced by mass spectrometry can act as a fingerprint for each protein or peptide, and help in identification when compared to a database.

Attempts to purify LL-37 by gel electrophoresis were made problematic due to the small size and low abundance of the peptide in patient plasma. The size of the mature peptide (4.5 kDa) made traditional Laemmli SDS-PAGE gels unsuitable, so the Tris-Tricine method was employed, as these gels achieve better separation of low molecular weight proteins. To further increase this separation, the use of highly concentrated gels (12.5 to 16%) and a higher cross linking percentage were suggested[57].

Figure 3.6 shows an image of a 16% Tris-Tricine gel with 3% cross-linking. Lanes 8-9 show the necessity for purification steps prior to electrophoresis, as the abundant plasma protein albumin masks other high molecular weight bands, and distorts those of a low molecular weight. Lanes 4-7 show reasonably good separation and resolution, and a number of bands were extracted for subsequent mass spectrometric analysis. However, as indicated by their faintness, these bands were of low abundance peptides, and did not produce significant database hits. In addition, bands in the LL-37 standard lanes (2-3) appeared at a higher mass than would be expected (arrows 2 and 3), suggesting the presence of material other than the antimicrobial peptide (e.g. some form of preservative).

As LL-37 is processed from a precursor (hCAP-18), which has a molecular weight of 16-18 kDa, sample bands of around this size were also extracted for analysis by MALDI-TOF. Bands of an appropriate size were

identifiable in the Tris-Tricine gels (e.g. Figure 3.6, arrow 1), but did not produce significant hits when the spectra were compared to a database.
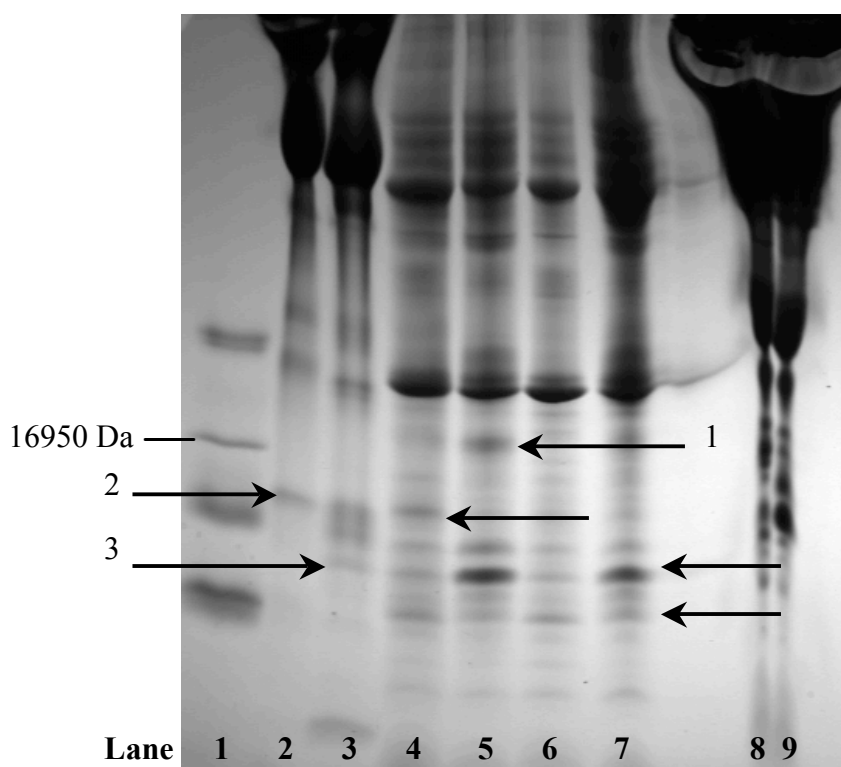
Figure 3.6 – 16% Tris-Tricine gel with 3% cross-linking
Arrows indicate bands extracted for MALDI analysis

Lane 1: 10 μL ladder; Lane 2: 10 μL LL-37 standard (1:1 with GLB); Lane 3: 10 μL LL-37 standard with 0.2 μg/μL formic acid (1:1 with GLB); Lane 4-7: 10 μL sample (albumin removal/TCA pellet resuspended in 40 μL water, 1:1 with GLB, supernatant loaded); Lane 8-9: 10 μL sample plasma (1:1 GLB)

As shown in Figure 3.7a, the methanol/acetic acid (Me/Ac) precipitation method for plasma purification did not produce the same clean banding pattern as the albumin removal and TCA precipitation method (Figure 3.7b). This may have been because the albumin was not specifically removed in the Me/Ac method, so could have impacted the resolution of other bands.

a)

b)
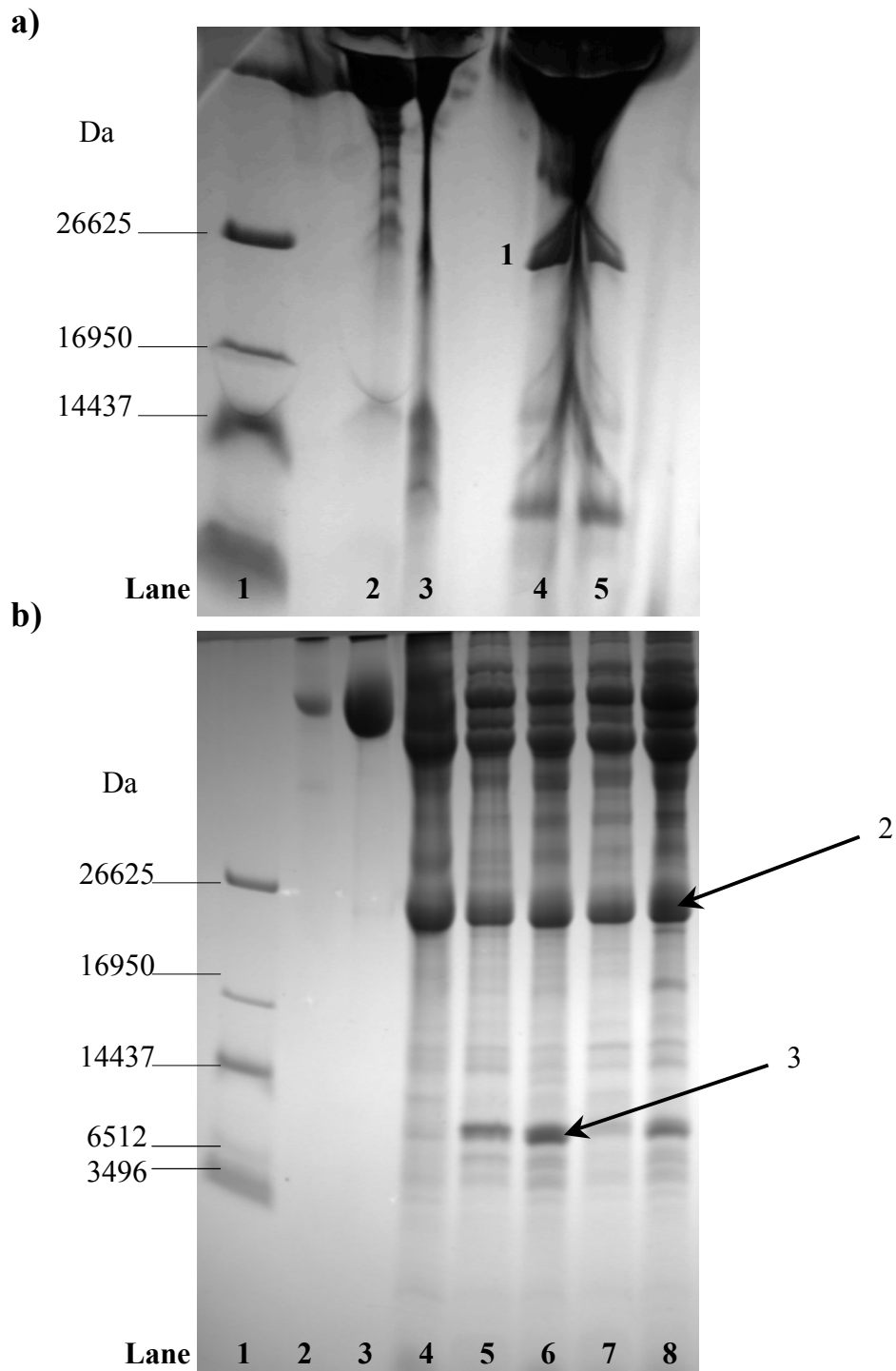
Figure 3.7 – 16% Tris-Tricine gel with 3% cross-linking, blue-silver stained

a) Lane 1: 20 μL ladder; Lane 2: 20 μL LL-37 standard (100 μL dried in SpeedVac plus 30 μL GLB); Lane 3: 20 μL LL-37 with 0.2 μg/μL formic acid (2:1 with GLB); Lane 4-5: 20 μL samples (Me/Ac precipitated, in 50μL GLB)

b) Lane 1: 10 μL ladder; Lane 2: 10 μL LL-37 standard (2:1 with GLB); Lane 3: hBD-2 standard (2:1 with GLB), Lane 4-8: 10 μL samples (albumin removal/TCA pellet in 40 μL water, 1:1 with GLB, supernatant loaded)

Regardless of the purification technique used, MALDI analysis only produced positive identifications for the most abundant peptides present in the fraction submitted to gel electrophoresis. These were apolipoprotein A-I and serum amyloid A protein (SAA1), the most significant hits for which are displayed in Table 3.3.

Table 3.3 – Positive identifications and significance levels from MALDI-TOF analysis of bands extracted from Tris-Tricine gels

Hit	Molecular weight (Da)	Mascot score (>73 for significance)	Figure showing band
Apolipoprotein A-I gi/90108664	28061.470	352	Figure 3.7a (band 1)
		155	Figure 3.7b (band 2)
Serum amyloid A1 gi/13937839	13524.500	110	Figure 3.7b (band 3)

See Appendix 6.4 for full MALDI results

An interesting observation is that the ladder appears to run slightly higher than the samples. For example, in Figure 3.7b, the apolipoprotein band of approximately 28 kDa was positively identified below the highest molecular weight band of the ladder (triosephosphate isomerase, ~26 kDa). This suggests that potential LL-37 bands may actually be further down the gel than expected. In addition, not all bands of the ladder were always seen with blue-silver staining.

Figure 3.8 shows a comparison of blue-silver (a) and silver (b) staining on the same 16% Tris-Tricine gel. Silver staining allowed visibility of more sample bands, and the two lowest molecular weight ladder bands, which could not be seen with blue-silver. However, even with this increased stain sensitivity, only faint bands were seen in the LL-37 standard lane, and only one of these (indicated by an arrow) appeared near the expected molecular weight.
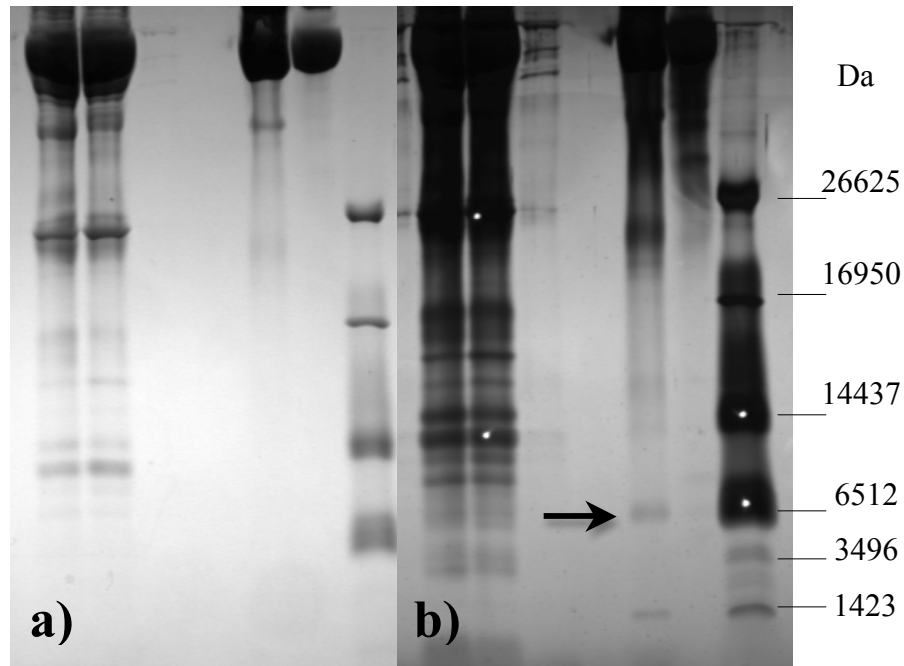
Figure 3.8 – 16% Tris-Tricine gel with 6% cross-linking, stained with blue-silver (a) and silver (b)
(Arrow indicates potential LL-37 band in standard lane)

3.6   Lysozyme gels

A range of concentrations of lysozyme were run on small 16% Tris-Tricine gels, to determine the concentration threshold for detection by blue-silver staining. The lowest protein load visible was 1 ng, with a possible faint band at 0.5 ng (Figure 3.9). Even fainter band-like patterns can also be seen in the control lane (0 ng) and in the 0.1 ng lane, suggesting heavy well loading may have caused splash-over into other wells and produced bands where lysozyme would otherwise not have been detected. This conclusion is supported by the fact that the group responsible for developing this staining protocol reported a detection limit of 1 ng, with the possibility of 0.75 ng as the minimal detectable load for BSA[62]. In addition, this low detection was not reproducible in the current study, as several repeats of the experiment failed to produce bands at loads of below 100 ng.

Load (ng):	0	1000	500	100	50	10	5	1	0.5	0.1
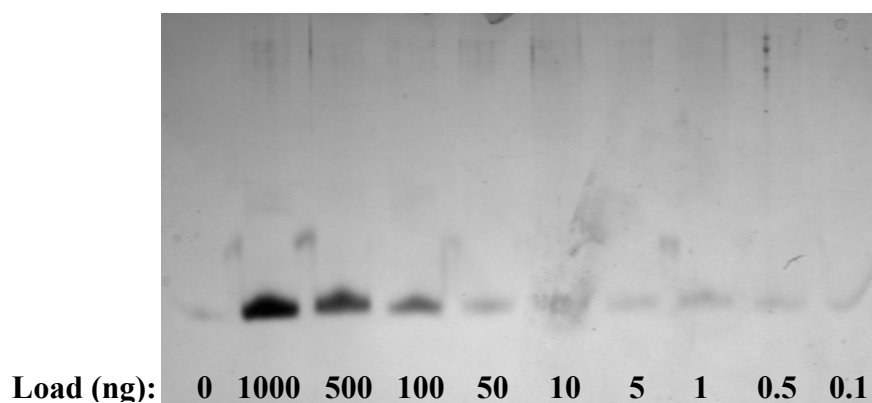
Figure 3.9 – 16% Tris-Tricine gel with 3% cross-linking, showing detection limit for blue-silver staining

MALDI-TOF mass spectrometry has been reported to be capable of detection at the subpicomole level. This high sensitivity relies on sample purity, and the electrophoretic separation of the diversity of proteins in plasma is therefore a very important preparative step. However, separation is only useful if the protein or peptide of interest can be detected and extracted from the gel. This means that, if the stain used cannot visualise the desired protein, the sensitivity of the MALDI becomes irrelevant[63].

One method that enables a lower detection limit to be reached is silver staining, which can visualise protein loads of down to 1-10 ng. However, it is widely accepted that this technique is unsuitable in cases where subsequent MALDI-TOF mass spectrometry of the stained proteins is required. This incompatibility results from the use of Ag^+ and sensitizing agents (particularly glutaraldehyde), which can cause protein destruction or modification, and thereby impede protein identification[64].

Two other techniques were performed on gels with the same lysozyme concentration gradient, to determine whether the detection threshold could be lowered, while improving MALDI compatibility through slight modifications of the silver staining protocol. However, these methods did not improve detection over that of the blue-silver stain, and had poorer band resolution (results not shown).

Another suggestion for improving the MALDI results was to increase the amount of material subjected to analysis. Taking single plugs from each band for tryptic digestion and mass spectrometry was compared to whole band extraction, to see if more material allowed for better detection, or whether the background

was also increased. Single plug/whole band comparison was carried out for dried droplet and thin layer target loading techniques, to determine which method produced better peak resolution. Inclusion of a wash step improved the spectra for both dried droplet and thin layer techniques, and the thin layer/wash method produced the highest peak intensity overall, particularly when the whole band was used (Figure 3.10).
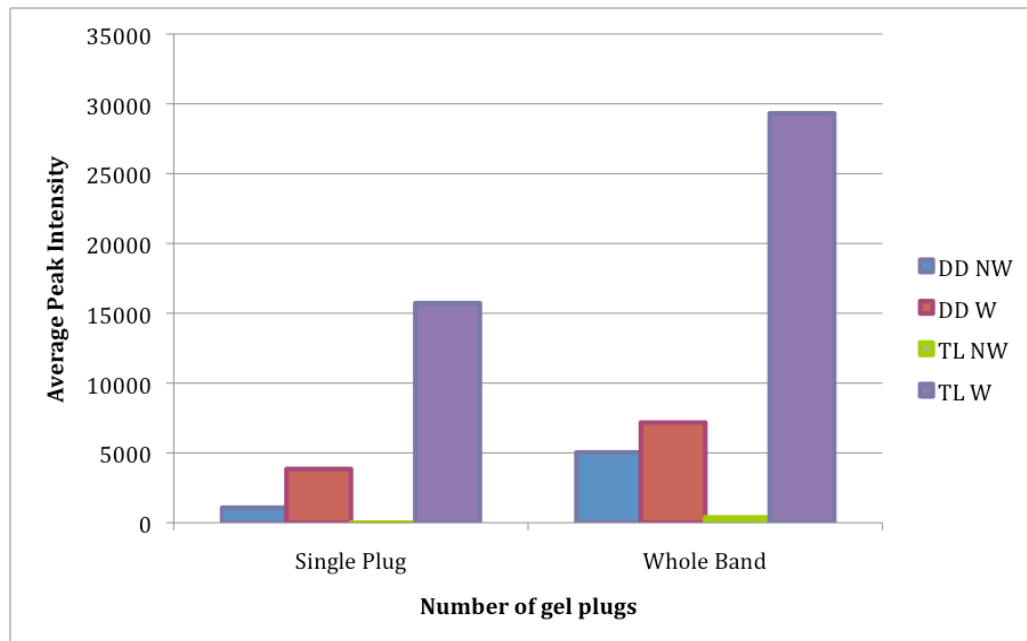
Figure 3.10 – Comparison of MALDI preparation techniques for single plug and whole band extraction from Tris-Tricine gels
DD – dried droplet; TL – thin layer; NW – no wash; W – wash

3.7   Discussion of Tris-Tricine SDS-PAGE and MALDI-TOF of LL-37

Despite using the Tris-Tricine method, high gel concentrations, increased cross-linker percentage, more sensitive staining procedures and different mass spectrometry target-laying techniques, LL-37 could not be isolated by gel electrophoresis and identified by MALDI-TOF. This prevented further development of the plasma screening method because, although the sample spectra contained peaks that resembled those seen in the standard, it could not be confirmed that they were the peaks of interest.

The low abundance of LL-37 caused problems in this study; particularly as the maximum concentration measured in the patient cohort only reached 341.25 ng/mL. This is substantially lower than the 1.2-1.8 μg/mL that has been

reported in plasma, and it is uncertain why the patient levels were so reduced. One possibility is that the concentration was reported in the context of the precursor protein (hCAP-18), while the mature peptide (LL-37) was measured in the present study. Alternatively, as LL-37 is the active antimicrobial peptide and is involved in the innate immune response, it may have become depleted in the study patients as a result of consumption during infection.

Further development of this method may require western blots to be employed, to allow more sensitive detection than the 100 ng limit observed for blue-silver and modified silver staining. The specificity of antibodies used in western blots may help combat the low plasma levels of this peptide being a barrier to detection.

Only two proteins could be positively identified by MALDI – SAA1 and apolipoprotein A-I, both of which are of much higher abundance than LL-37[65]. Of particular interest to this study is apolipoprotein A-I, which is thought to sequester LL-37 in the bloodstream. The presence of this protein in these gels lends support to the assumption that LL-37 was not removed during the purification procedures.

Effective isolation of LL-37 from other plasma proteins (particularly those of greater abundance) is likely to lead to successful identification of the peptide by mass spectrometry. This is because proper separation would produce a much purer extract for use in MALDI, which would allow the high sensitivity of the instrument to be utilised.

Once the identity of the LL-37 peaks has been confirmed, the next step in developing the plasma screening method would be to trial different target loading techniques. If the sample distribution on the target is not homogenous, proteins (including LL-37) may clump together to form "hot spots", while other regions will largely be composed of matrix. In these cases, directing the laser at different parts of the target spot yields significantly different spectra, as all the sample becomes localised. This would complicate determination of the threshold for detection of LL-37. An homogenous distribution however, would allow representative spectra to be collected from any point on the target. This would allow the threshold be identified more easily, and it could be determined with confidence whether a sample fell above or below this level, which is the basis for the clinical utility of this method.

3.8   DBP polymorphism determination by PCR, a pilot study

During the course of this research project, a paper was published by Fu *et al.*[47] that reported differences in serum 25-hydroxyvitamin D_3 (25D) levels in individuals with polymorphic variants of the vitamin D binding protein (DBP) gene. These polymorphisms were also shown to influence the effectiveness of vitamin D supplementation. As the variants have been identified in a wide range of ethnic groups, influence vitamin D levels, and are possible candidates for the genetic factor predisposing certain individuals to COPD, these findings had important implications for this study.

Unfortunately, the application approved by the Northern Y ethics committee did not cover the use of patient DNA. Extension of this approval to include DNA work would have required further patient consent, and was therefore not obtainable within the time constraints of this project. Instead, twenty volunteers from the University of Waikato research laboratories supplied DNA (via a saline mouthwash), which was genotyped to identify DBP polymorphisms. The purpose of this pilot study was to determine whether the same variants were present in a New Zealand population, and to develop a method that could later be used to identify DBP genotypes in the study patients.

The method of Fu *et al.* used a mutant reverse primer that was designed in such a way as to make mutant (K allele) bands 21 bp longer (270 bp) than wild-type bands (249 bp). In practice however, it was extremely difficult to distinguish the two alleles, so the majority of heterozygotes were overlooked and could only be identified through subsequent sequencing. Figure 3.11 shows a 2% PCR gel with heterozygotes in lanes 1, 3 and 4, where a faint mutant band can be seen. However, this was the only gel in which these could be identified, and sequencing every sample would have been costly and impractical.
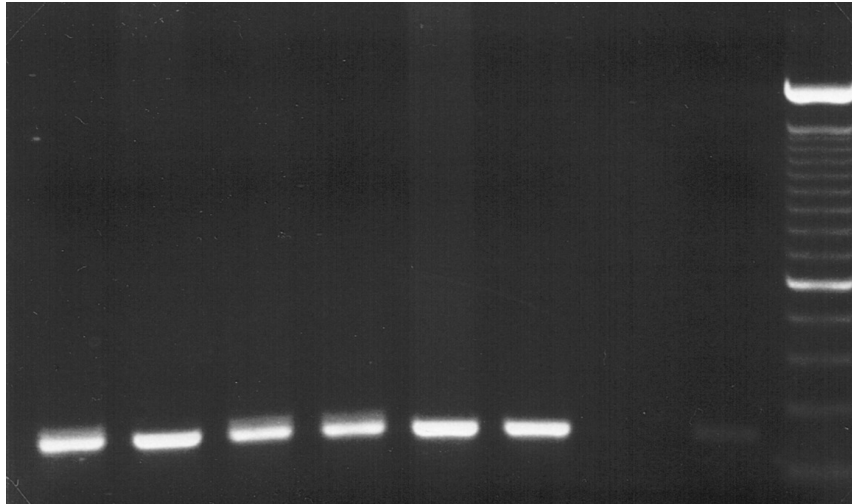
Figure 3.11 – 2% Agarose/1x TAE gel of PCR-amplified DBP products, multiplex system
(From left: TK, TT, TK, TK, TT, TT, x, negative, 100 bp ladder)

It was suggested that running the PCR reaction as a multiplex was causing the mutant bands to appear faint, perhaps as a result of more efficient amplification by wild-type primers. This could not be confirmed however, as carrying out a separate PCR reaction for each sample (i.e. one using the wild-type reverse primer and the other using the mutant) also produced gels with faint mutant bands (Figure 3.12).
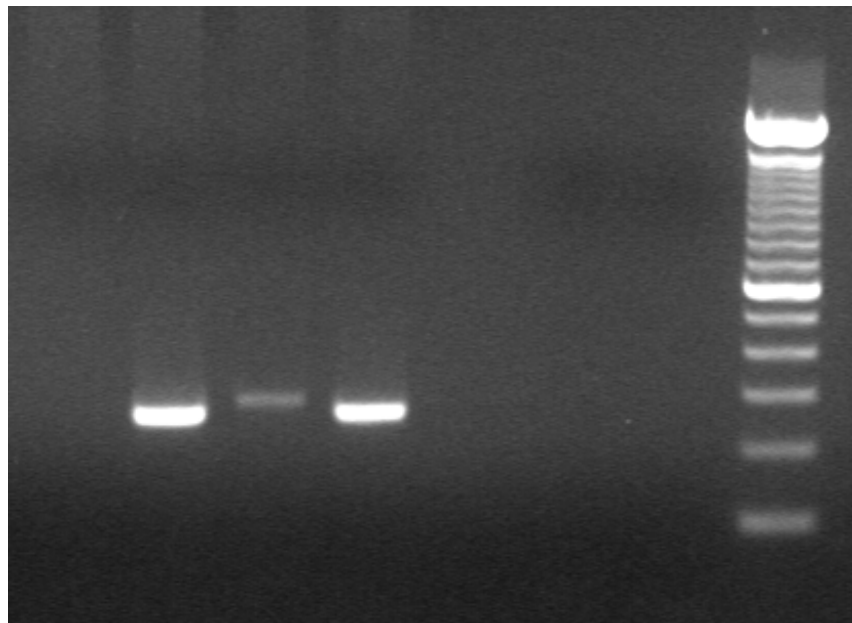
Figure 3.12 – 2% Agarose/1x TAE gel of PCR-amplified DBP products, duplex system
(From left: TT mutant, TT wild-type, TK mutant, TK wild-type, x, mutant negative, wild-type negative, 100 bp ladder)

To improve the method, alternative PCR conditions were used in an attempt to increase the brightness of the mutant bands, to at least match that of the wild-type. The touchdown protocol effectively produced the desired resolution, and Figure 3.13 shows a gel with an example of each genotype (i.e. TT, TK and KK).
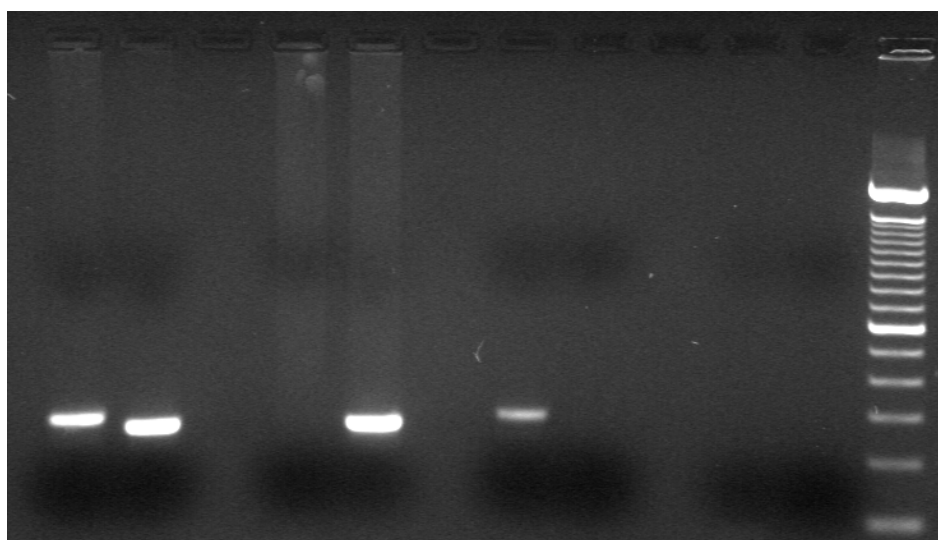
Figure 3.13 – 2% Agarose/1x TAE gel of touchdown PCR products
(From left: TK mutant, TK wild-type, x, TT mutant, TT wild-type, x, KK mutant, KK wild-type, x, mutant negative, wild-type negative, 100 bp ladder)

The T436K results of this study and those of Fu *et al.* are shown in Table 3.4, and both identified the homozygous KK genotype as the most rare. However, TK had the highest frequency in this study, while Fu *et al.* found TT to be the most common.

Table 3.4 – Comparison of T436K and D432E allele frequencies from this study and that of Fu *et al.*

SNP	Alleles	Pilot study allele frequency (n=20)	Fu *et al.* allele frequency (n=98)
T436K	TT	7 (35%)	50 (51%)
	TK	12 (60%)	33 (34%)
	KK	1 (5%)	6 (6%)

Samples were also subjected to HaeIII digestion, to determine the D432E genotype. The recognition site for this enzyme was only present in the E allele sequence, meaning that D bands remained uncut. As the PCR gels of all but one individual showed a T allele band, the PCR-amplified mixtures from the wild-type reactions were used for the restriction enzyme digestion. Therefore, homozygous DD individuals retained the 249 bp band, which was cut into two bands (221 and 28 bp) in EE homozygotes, and all 3 bands were present in heterozygous (DE) individuals (Figure 3.14).

Note: in the KK individual, the mutant band was used instead, with expected band sizes of 270 bp (DD), 221 and 49 bp (EE), and 270, 221 and 49 bp (DE).
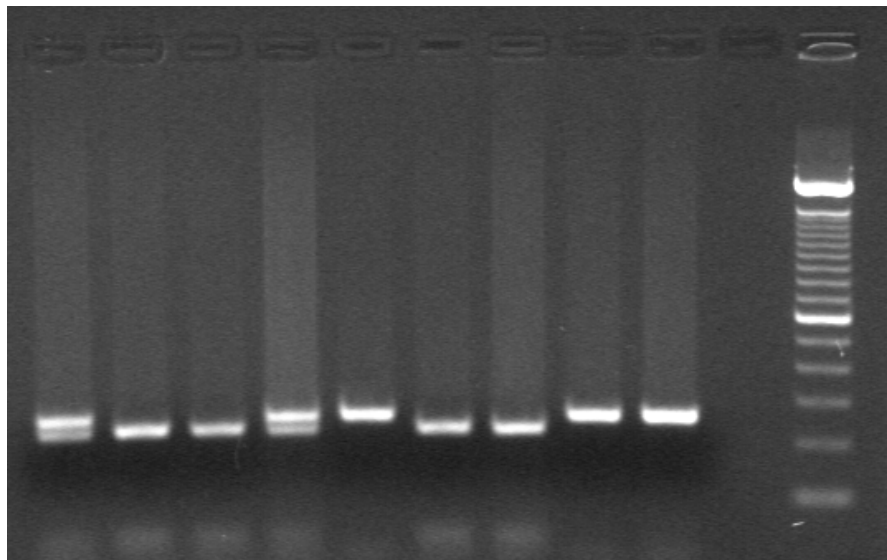
Figure 3.14 – 2% Agarose/1x TAE gel of HaeIII-digested PCR products
From left: DE, EE, EE, DE, DD, EE, EE, DD, DD, x, 100 bp ladder

Four samples (two from the multiplex method and two from touchdown) were sequenced to ensure the whole and restriction enzyme-digested bands were representative of the correct genotypes. This sequencing confirmed the gel results for T436K (for sequences and electropherograms, see Appendix 6.5). However, examination of the touchdown wild-type and mutant sequences of a TK individual revealed that this technique is only sufficient for the D432E genotyping of TT homozygotes. This is because, if only the T band is analysed in TK individuals, D432E variation in the mutant band is ignored, and heterozygotes become overlooked. This would also be expected when examining these genotypes in the

multiplex system, as the restriction enzyme digestion of the faint mutant band is unlikely to be visible on the gel, in the presence of the much brighter wild-type bands.

Based on this realisation, the true D432E genotype of all but one of the TK individuals (11 of 20 samples) could not be determined without further analysis, either by HaeIII digestion of the K band, or by sequencing. Fu et al.[47] indicated that the D432E genotype was not significantly associated with serum vitamin D levels, and is therefore not as relevant to this study as the T436K genotype. However, for completeness, allele frequencies of the 9 samples with valid D432E genotyping (i.e. TT, KK and sequenced TK individuals) are displayed in Table 3.5 and, despite their low sample numbers, these frequencies are reasonably consistent with those of the Fu et al. study.

Table 3.5 – Comparison of D432E allele frequencies from this study and that of Fu et al.

SNP	Alleles	Pilot study allele frequency (n=9)	Fu et al. allele frequency (n=98)
	DD	2 (22%)	22 (22%)
D432E	DE	5 (56%)	41 (42%)
	EE	2 (22%)	26 (27%)

3.9   Proteomic approach for identification of DBP genotype

As an alternative to DNA work, a proteomic approach was employed in an attempt to distinguish Gc1 and Gc2 genotypes in a way that remained within the approved ethical guidelines. This approach was based on the work of Kitchin and Bearn[66], who demonstrated the ability to identify Gc1-1, 1-2 and 2-2 genotypes through the use of polyacrylamide gels, as each produces a different banding pattern, as shown in Figure 3.15.
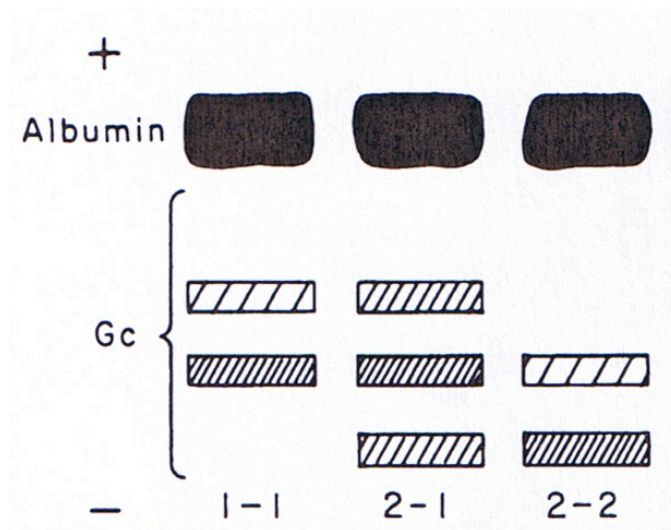
Figure 3.15 – Banding patterns expected for different Gc-globulin genotypes, as published by Kitchin and Bearn[66]

The molecular weight of the DBP protein (~51 kDa) made the use of Laemmli gels more suitable than the Tris-Tricine method. Figure 3.16 shows a photo of a 7% Laemmli gel loaded with 2.5 μL plasma (diluted 1:50 in GLB) per well, and 20 μL ladder (Bio-Rad Precision Plus Protein Standards (Dual Colour), 161-0374).

kDa
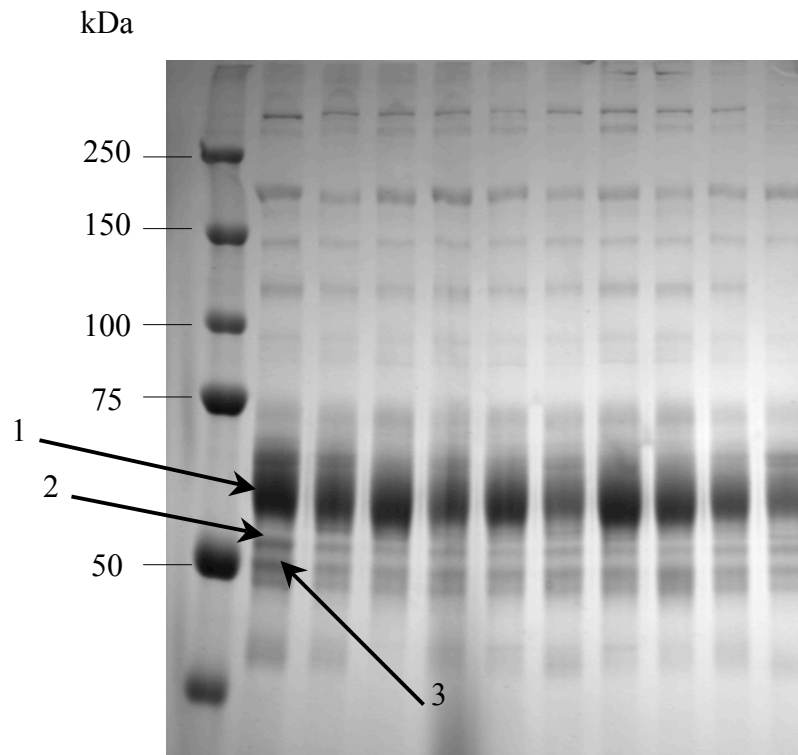
**Figure 3.16 – 7% Laemmli gel of diluted plasma samples, arrows indicate
bands extracted for MALDI analysis**

Albumin has a molecular weight of approximately 66 kDa, and is the most
abundant protein in human serum, constituting about 50% of the total protein
content. This is increased to over 95%, when the other eleven high abundance
proteins are also included[65]. Therefore, the huge diversity of proteins found in
serum falls largely within the remaining 5%, indicating that they are of relatively
low abundance. A paper by Hortin *et al.*[65] ranked 150 proteins according to the
amounts present in healthy human plasma. Among the top ten were albumin,
various immunoglobulins, apolipoprotein A-I (see section 3.7), and fibrinogen.
Gc-globulin was ranked 25th, with a concentration of 8-14 μmol/L. Although
listed quite highly in terms of abundance, these levels are relatively low when
compared to the 500-800 μmol/L of albumin.

Table 3.6 shows the Mascot hits for the bands indicated in Figure 3.16.
Three significant hits were obtained for band 1, and all indicate that it is likely to
be albumin, as expected based on the molecular weight and intensity. Although it
does not have the highest score, the molecular weight of hit 3 is closest to that
expected. Bands 2 and 3 were identified as being related to fibrinogen. As the β-

chain of fibrinogen was ranked 18th by Hortin *et al.* with a concentration of 10-27 µmol/L, all the proteins identified were of higher abundance than Gc-globulin. Based on the molecular weights of these bands, Gc-globulin should be in the same area, between albumin and fibrinogen β-chain (i.e. bands 1 and 2).

Table 3.6 – Positive identifications and significance levels from MALDI-TOF analysis of bands extracted from Laemmli gels

Hit	Molecular weight (Da)	Mascot score (>73 for significance)	Figure showing band
Hit 1: **Albumin-like** gi/763431	52048	91	Figure 3.16 (band 1)
Hit 2: **Albumin, isoform CRA_t [Homo sapiens]** gi|119626083	58614	86	
Hit 3: **Chain A, Structure Of Human Serum Albumin With S-Naproxen And The Ga Module** gi|168988718	65778	86	
Fibrinogen beta chain, isoform CRA_f [Homo sapiens] gi|119625340	44153	82	Figure 3.16 (band 2)
Chain C, Crystal structure of recombinant human fibrinogen fragment D gi|24987625	35155	82	Figure 3.16 (band 3)

See Appendix 6.4 for full MALDI results

As the Gc-globulin bands run so close to albumin, gradient gels of 7-10% were used as a means of increasing separation. However, this closeness made it

extremely difficult to run the gel in such a way as to distribute the Gc bands in the lower percentage section, while retaining albumin in the 10% separating gel. Despite this, one such gradient gel did produce some Gc-like banding, which can be seen in the magnified section of Figure 3.17. Arrow 1 indicates a cluster of three bands (although difficult to distinguish from each other in the photo), which could represent an individual with the Gc1-2 genotype. The two bands indicated by arrow 2 appear in line with the upper and middle of the three bands, indicative of Gc1-1. However, this could not be confirmed by subsequent MALDI analysis.
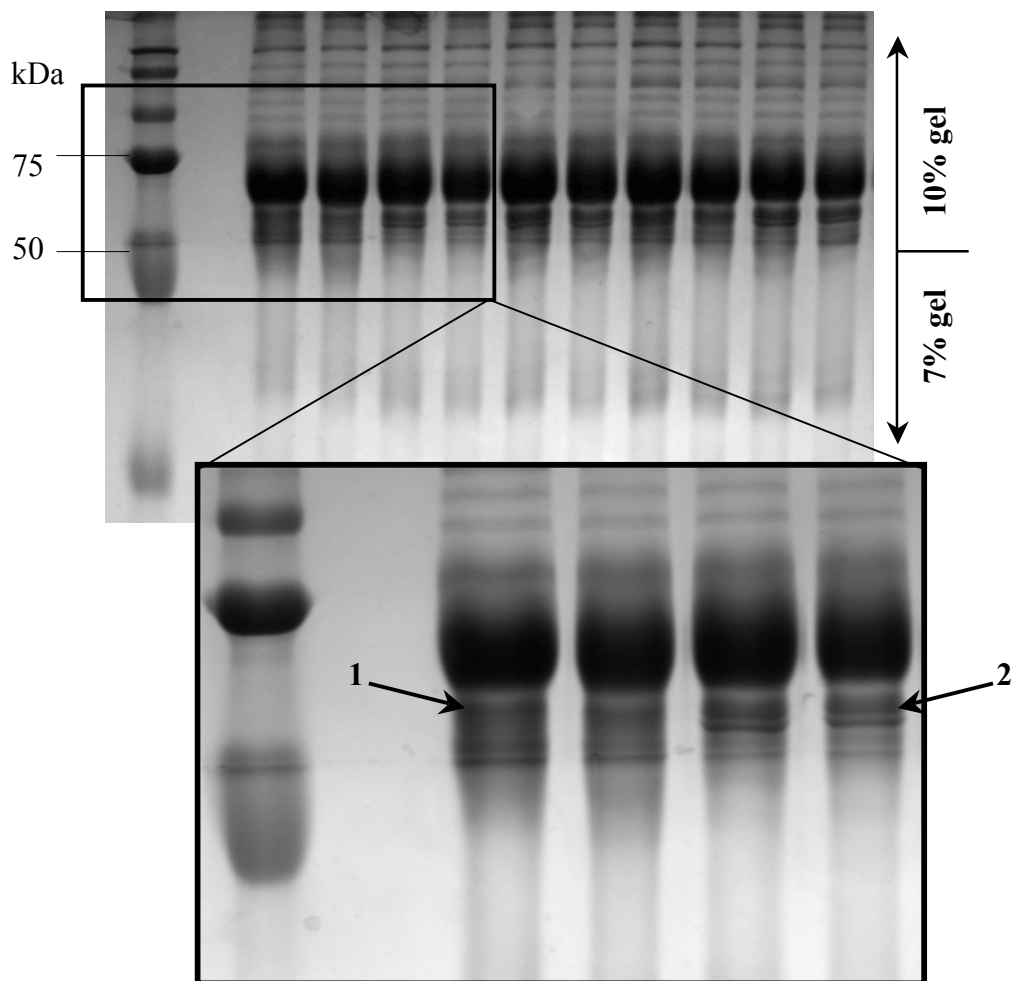
Figure 3.17 – Gradient gel of diluted plasma samples showing increased magnification of relevant section

Although a significant improvement over the single concentration separating gel (Figure 3.16), this resolution would need to be further improved before the polymorphic variants could be confidently identified. This may include

the incorporation of a purification step before gel electrophoresis, such as that used by Christiansen *et al.*[44], which allowed the successful isolation of Gc-globulin from plasma. However, this group used a large-scale method, which was not practical for this study, as comparison of small volumes of patient plasma was required. Alternatively, band resolution could be increased if a step for the removal of albumin was included. As DBP is a member of the same superfamily as albumin, this step would have to be highly specific, to prevent the removal of both proteins.

More recent proteomic methods for identifying Gc-globulin variants tend to involve immunoelectrophoresis or isoelectric focussing. However, these methods require the purchase of specific antibodies that are able to distinguish between each Gc isoform, to allow visualisation of the different variants. The most effective method in terms of results, simplicity, and sample throughput was PCR; so future work on this study should aim to gain ethical approval for analysing DBP polymorphisms using patient DNA.

The only real difficultly with using the stored plasma samples for PCR is the extraction of DNA. However, the recently published method of Xue *et al.*[67] was found to be effective in the isolation of cell-free DNA, such as that contained in plasma.

4. Conclusions

The health benefits of vitamin D have been studied for a long time. Until recently however, these studies have largely focussed on its role in maintaining bone health and skeletal integrity, particularly in relation to the prevention of rickets in children. This involvement in bone metabolism is now well known, and is commonly referred to as the main function of the vitamin. More recent findings, such as those indicating the widespread distribution of vitamin D receptors in the body, and the correlation between latitude and incidence rates for a number of diseases, have inspired renewed interest in this hormone, and led to the discovery of its involvement in a multitude of other biological processes.

The aim of this research was to explore the relationship between the plasma levels of vitamin D and the antimicrobial peptides LL-37 and hBD-2 in patients with pneumonia or exacerbations of COPD. Many studies have indicated that vitamin D plays a role in the regulation of such peptides via response elements in the gene promoters, so it was hypothesized that 25D levels would correlate with peptide concentration. As these peptides constitute an essential part of the innate immune response, it was also hypothesized that individuals with reduced peptide production would suffer from more severe infection (i.e. higher CURB65 scores) and have a greater risk of mortality. Although these hypotheses where not supported by the results, this research did produce several important findings.

Firstly, the finding that severe vitamin D deficiency (i.e. <30nmol/L) was significantly associated with increased mortality in both infections, has important implications for clinical treatment, as it suggests that vitamin D supplementation has the potential to reduce the risk of death. Further research would be required to identify the precise 25D threshold below which survival becomes reduced, and clinical trials could help determine whether boosting these levels would bring about the expected drop in mortality.

Secondly, to the best of my knowledge, this is the first study to identify a relationship between LL-37 and mortality in COPD, and studies designed to ascertain whether boosting these levels could aid in treatment would also be valuable.

Further development of the MALDI-TOF screening method could be useful in the meantime, to help rapidly identify patients most at risk of death. Based on this research, the main barrier to the success of this method was the detection of LL-37 after electrophoretic separation. None of the methods employed here allowed visualisation of this small, low abundance peptide, which prevented effective isolation for mass spectrometry. Future work should focus on using antibodies for detection, as the levels in the patient plasma are particularly low.

Both vitamin D and LL-37 seem to be significant determinants of mortality in these diseases, where low levels increase the risk in both cases. Based on the lack of association between the two variables however, their effects on survival appear to be independent. Further research into the interplay between vitamin D and LL-37 in the context of these infections would be interesting, as the presence of VDREs in the cathelicidin gene promoter, and the ability of vitamin D to upregulate expression of the AMP *in vitro* suggest some form of connection must exist. It seems possible that LL-37 could be associated with active 1,25D, and that its relationship with 25D is therefore indirect.

Another aspect worthy of further attention is the vitamin D binding protein (DBP). It would be interesting to use the PCR method developed in this project to assess the DBP polymorphisms of the study patients for two main reasons. Firstly, the DBP genotype Gc1F is thought to predispose its carriers to COPD, while the Gc2-2 genotype is believed to be protective. Analysis of the frequency of each isoform in the COPD group would allow determination of whether such a relationship exists in this cohort, or whether these associations are population-specific.

More relevant to the study group as a whole, would be to compare the T436K genotype with 25D levels to determine whether baseline vitamin D is influenced, as suggested by Fu *et al.*[47] This SNP is also thought to influence how an individual will respond to vitamin D supplementation which, coupled with the finding that low vitamin D increases rates of mortality, has a broader relevance to this study. Integrated clinical studies incorporating both of these findings would have to be employed to prevent the production of erroneous results. That is, when determining if vitamin D supplements can reduce mortality in these respiratory

infections, they would have to be administered based on DBP genotype, to account for differences in subject responses.

In this modern world of increasing antibiotic resistance and the everlasting search for new therapeutic drugs, it is somewhat ironic that it be compounds such as vitamin D and antimicrobial peptides – products synthesised by the body and studied for many years, that would prove to be of such integral importance to human survival, and the subject of renewed interest on a seemingly exponential scale. This study provides yet another context in which they show significance, and presents findings that suggest potential clinical importance for these natural antibiotics and the "sunshine vitamin".

5. References

1.   Holick, M. F. (2004). Sunlight and vitamin D for bone health and prevention of autoimmune diseases, cancers, and cardiovascular disease. *American Journal of Clinical Nutrition* **80**, 1678-1688.

2.   Mandavilli, A. (2007). The sunshine cure. *Nature Medicine* **13**, 396-397.

3.   Cavalier, E., Delanaye, P., Chapelle, J. & Souberbielle, J. (2009). Vitamin D: current status and perspectives. *Clinical Chemistry and Laboratory Medicine* **47**, 120-127.

4.   Mora, J. R., Iwata, M. & von Andrian, U. H. (2008). Vitamin effects on the immune system: vitamins A and D take centre stage. *Nature Reviews* **8**, 685-698.

5.   Holmes, A. D., Pigott, M. G., Sawyer, A. & Comstock, L. (1932). Vitamins aid reduction of lost time in industry. *Industrial and Engineering Chemistry* **24**, 1058-1060.

6.   Kimlin, M. G. (2008). Geographic location and vitamin D synthesis. *Molecular Aspects of Medicine* **29**, 453-461.

7.   Segaert, S. (2008). Vitamin D regulation of cathelicidin in the skin: toward a renaissance of vitamin D in dermatology? *Journal of Investigative Dermatology* **128**, 773-775.

8.   Deeb, K. K., Trump, D. L. & Johnson, C. S. (2007). Vitamin D signalling pathways in cancer: potential for anticancer therapeutics. *Nature Reviews* **7**, 684-697.

9.   White, J. H. (2008). Vitamin D signaling, infectious diseases, and regulation of innate immunity. *Infection and Immunity* **79**, 3937-3843.

10.   Diamond, T. H., Eisman, J. A., Mason, R. S., Nowson, C. A., Pasco, J. A., Sambrook, P. N. & Wark, J. D. (2005). Vitamin D and adult bone health in Australia and New Zealand: a position statement. *MJA* **182**, 281-285.

11.   Grant, W. B. & Holick, M. F. (2005). Benefits and requirements of vitamin D for optimal health: a review. *Alternative Medicine Review* **10**, 94-111.

12.   Janssens, W., Lehouck, A., Carremans, C., Bouillon, R., Mathieu, C. & Decramer, M. (2009). Vitamin D beyond bones in chronic obstructive pulmonary disease. *Am J Respir Crit Care Med* **179**, 630-636.

13.   Rockell, J. E. P., Skeaff, C. M., Williams, S. M. & Green, T. J. (2006). Serum 25-hydroxyvitamin D concentrations of New Zealanders aged 15 years and older. *Osteoporosis International* **17**, 1382-1389.

14.   Muhe, L., Lulseged, S., Mason, K. E. & Simoes, E. A. F. (1997). Case-control study of the role of nutritional rickets in the risk of developing pneumonia in Ethiopian children. *The Lancet* **349**, 1801-1804.

15.   DeSmet, K. & Contreras, R. (2005). Human antimicrobial peptides: defensins, cathelicidins and histatins. *Biotechnology Letters* **27**, 1337-1347.

16.   Nelson, R. J., Demas, G. E., Klein, S. L. & Kriegsfeld, L. J. (2002). *Seasonal patterns of stresses, immune function, and disease*, Cambridge University Press.

17.   Boman, H. G. (2003). Antibacterial peptides: basic facts and emerging concepts. *Journal of Internal Medicine* **254**, 197-215.

18.   Bulet, P., Stöcklin, R. & Menin, L. (2004). Antimicrobial peptides: from invertebrates to vertebrates. *Immunological Reviews* **198**, 169-184.

19.   Nizet, V. & Gallo, R. L. (2003). Cathelicidins and innate defense against invasive bacterial infection. *Scandanavian Journal of Infectious Disease* **35**, 670-676.

20.   Ulrich, H. N., Sudheendra, U. S. & Ramamoorthy, A. (2006). LL-37, the only human member of the cathelicidin family of antimicrobial pepties. *Biochimica et Biophysica Acta* **1758**, 1408-1425.

21.   Hancock, R. E. W. & Diamond, G. (2000). The role of cationic antimicrobial peptides in innate host defences. *Trends in Microbiology* **8**, 402-410.

22.   Zanetti, M., Gennaro, R. & Romeo, D. (1995). Cathelicidins: a novel protein family with a common proregion and a variable C-terminal antimicrobial domain. *FEBS Letters* **374**, 1-5.

23.   Tjabringa, G. S., Rabe, K. F. & Hiemstra, P. S. (2005). The human cathelicidin LL-37: a multifunctional peptide involved in infection and inflammation in the lung. *Pulmonary Pharmacology and Therapeutics* **18**, 321-327.

24.   Sørensen, O. E., Bratt, T., Johnsen, A. H., Madsen, M. T. & Borregaard, N. (1999). The human antibacterial cathelicidin, hCAP-18, is bound to lipoproteins in plasma. *The Journal of Biological Chemistry* **274**, 22445-22451.

25.   Wang, Y., Agerberth, B., Löthgren, A., Almstedt, A. & Johansson, J. (1998). Apolipoprotein A-I binds and inhibits the human

antibacterial/cytotoxic peptide LL-37. *The Journal of Biological Chemistry* **273**, 33115-33118.

26.   Sørensen, O. E., Follin, P., Johnsen, A. H., Calafat, J., Tjabringa, G. S., Hiemstra, P. S. & Borregaard, N. (2001). Human cathelicidin, hCAP-18, is processed to the antimicrobial peptide LL-37 by extracellular cleavage with proteinase 3. *Blood* **97**, 3951-3959.

27.   Oren, Z., Lerman, J. C., Gudmundsson, G. H., Agerberth, B. & Shai, Y. (1999). Structure and organization of the human antimicrobial peptide LL-37 om phospholipid membranes: relevance to the molecular basis for it non-cell-selective activity. *Biochemistry Journal* **341**, 501-513.

28.   Yang, D., Biragyn, A., Hoover, D. M., Lubkowski, J. & Oppenheim, J. J. (2004). Multiple roles of antimicrobial defensins, cathelicidins, and eosinophil-derived neurotoxin in host defense. *Annual Review of Immunology* **22**, 181-215.

29.   Cirioni, O., Giacometti, A., Ghiselli, R., Bergnach, C., Orlando, F., Silvestri, C., Mocchegiani, F., Licci, A., Skerlavaj, B., Rocchi, M., Saba, V., Zanetti, M. & Scalise, G. (2006). LL-37 protects rats against lethal sepsis caused by Gram-negative bacteria. *Antimicrobial Agents and Chemotherapy* **50**, 1672-1679.

30.   Kolls, J. K., McCray, P. B. & Chan, Y. R. (2008). Cytokine-mediated regulation of antimicrobial proteins. *Nature Reviews* **8**, 829-835.

31.   Ganz, T. (2003). Defensins: antimicrobial peptides of innate immunity. *Nature Reviews* **3**, 710-720.

32.   Fang, X.-M., Shu, Q., Chen, Q.-X., Book, M., Sahl, H.-G., Hoeft, A. & Stuber, F. (2003). Differential expression of α - and β -defensins in human peripheral blood. *European Journal of Clinical Investigation* **33**, 82-87.

33.   Cannell, J. J., Vieth, R., Umhau, J. C., Holick, M. F., Grant, W. B., Madronich, S., Garland, C. F. & Giovannucci, E. (2006). Epidemic influenza and vitamin D. *Epidermiol. Infect.* **134**, 1129-1140.

34.   Bals, R. & Hiemstra, P. S. (2004). Innate immunity in the lung: how epithelial cells fight against respiratory pathogens. *European Respiratory Journal* **23**, 327-333.

35.   Schutte, B. C. & McCray, P. B. (2002). β -defensins in lung host defense. *Annual Review of Physiology* **64**, 709-748.

36.   Hiratsuka, T., Nakazato, M., Date, Y., Ashitani, J., Minematsu, T., Chino, N. & Matsukura, S. (1998). Identification of human β -defensin-2 in respiratory tract and plasma and its increase in bacterial pneumonia. *Biochemical and Biophysical Research Communications* **249**, 943-947.

37. Schauber, J., Dorscher, R. A., Yamasaki, K., Brouha, B. & Gallo, R. L. (2006). Control of the innate epithelial antimicrobial response is cell-type specific and dependent on relevant microenvironmental stimuli. *Immunology* **118**, 509-519.

38. Liu, P. T., Stenger, S., Li, H., Wenzel, L., Tan, B. H., Krutzik, S. R., Ochoa, M. T., Schauber, J., Wu, K., Meinken, C., Kamen, D. L., Wagner, M., Bals, R., Steinmeyer, A., Zügel, U., Gallo, R. L., Eisenberg, D., Hewison, M., Hollis, B. W., Adams, J. S., Bloom, B. R. & Modlin, R. L. (2006). Toll-like receptor triggering of a vitamin D-mediated human antimicrobial response. *Science* **311**, 1770-1773.

39. Gombart, A. F., Bhan, I., Borregaard, N., Tamez, H., Camargo, C. A., Koeffler, P. & Thadhani, R. (2009). Low plasma level of cathelicidin antimicrobial peptide (hCAP18) predicts increased infectious disease mortality in patients undergoing hemodialysis. *Clinicial Infectious Diseases* **48**, 418-424.

40. Wang, T., Nestel, F. P., Bourdeau, V., Nagai, Y., Wang, Q., Liao, J., Tavera-Mendoza, L., Lin, R., Hanrahan, J. H., Mader, S. & White, J. H. (2004). Cutting edge: 1,25-dihydroxyvitamin D_3 is a direct inducer of antimicrobial peptide gene expression. *Journal of Immunology* **173**, 2909-2912.

41. Laaksi, I., Ruohola, J., Twohimaa, P., Auvinen, A., Haataja, R., Pihlajamäki, H. & Ylikomi, T. (2007). An association of serum vitamin D concentrations < 40 nmol/L with acute respiratory tract infection in young Finnish men. *American Journal of Clinical Nutrition* **86**, 714-717.

42. Sethi, S., Evans, N., Grant, B. J. & Murphy, T. F. (2002). New strains of bacteria and exacerbations of chronic obstructive pulmonary disease. *New England Journal of Medicine* **347**, 465-471.

43. Speeckaert, M., Huang, G., Delanghe, J. R. & Taes, Y. E. C. (2006). Biological and clinical aspects of the vitamin D binding protein (Gc-globulin) and its polymorphism. *Clinica Chimica Acta* **372**, 33-42.

44. Christiansen, M., Jørgensen, C. S., Laursen, I., Hirschberg, D., Højrup, P. & Houen, G. (2007). Protein chemical characterization of Gc globulin (vitamin D-binding protein) isoforms; Gc-1f, Gc-1s and Gc-2. *Biochimica et Biophysica Acta* **1774**, 481-492.

45. Meier, U., Gressner, O., Lammert, F. & Gressner, A. M. (2006). Gc-globulin: roles in response to injury. *Clinical Chemistry* **52**, 1247-1253.

46. Gaensslen, R. E. (1983). Group specific component. In *Sourcebook in forensic serology, immunology, and biochemistry*, pp. 581-586. Research Foundation of the City University of New York, New York.

47.   Fu, L., Yun, F., Oczak, M., Wong, B. Y. L., Vieth, R. & Cole, D. E. C.
       (2009). Common genetic variants of the vitamin D binding protein (DBP)
       predict differences in response of serum 25-hydroxyvitamin D [25(OH)D]
       to vitamin D supplementation. *Clinical Biochemistry* **42**, 1174-1177.

48.   Ishii, T., Keicho, N., Teramoto, S., Azuma, A., Kudoh, S., Fukuchi, Y.,
       Ouchi, Y. & Matsuse, T. (2001). Association of Gc-globulin variation with
       susceptibility to COPD and diffuse panbronchiolitis. *European
       Respiratory Journal* **18**, 753-757.

49.   Ito, I., Nagai, S., Hoshino, Y., Muro, S., Hirai, T., Tsukino, M. & Mishima,
       M. (2004). Risk and severity of COPD is associated with the group-
       specific component of serum globulin 1F allele. *Chest* **125**, 63-70.

50.   Schellenberg, D., Paré, P. D., Weir, T. D., Spinelli, J. J., Walker, B. A. M.
       & Sandford, A. J. (1998). Vitamin D binding protein variants and the risk
       of COPD. *American Journal of Critical Care Medicine* **157**, 957-961.

51.   Karalus, N. & Leow, L. (2009). (Simpson, T. M., ed.), Hamilton.

52.   Colantonio, D. A., Dunkinson, C., Bovenkamp, D. E. & Van Eyk, J. E.
       (2005). Effective removal of albumin from serum. *Proteomics* **5**, 3831-
       3835.

53.   Jiang, L., He, L. & Fountoulakis, M. (2004). Comparison of protein
       precipitation methods for sample preparation prior to proteomic analysis.
       Journal of Chromatography A **1023**, 317-320.

54.   McKenzie, J. L. (2006). A preliminary investigation of the application of
       MALDI-TOF mass spectrometry to biological systems, University of
       Waikato.

55.   Cole, A. M. & Ganz, T. (2000). Human antimicrobial peptides: Analysis
       and application. *BioTechniques* **29**, 822-831.

56.   Tang, Y., Yuan, J., Miller, C. J. & Selsted, M. E. (1999). Isolation,
       characterization, cDNA cloning, and antimicrobial properties of two
       distinct subfamilies of α -defensins fron Rhesus Macaque leukocytes.
       Infection and Immunity **67**, 6139-6144.

57.   Schägger, H. (2006). Tricine-SDS-PAGE. *Nature Protocols* **1**, 16-22.

58.   Coligan, J. E., Dunn, B. M., Ploegh, H. L., Speicher, D. W. & Wingfield,
       P. T., Eds. (1997). Current protocols in protein science. Vol. 1. United
       States of America: John Wiley and Sons, Inc.

59.   He, Q., Lau, G. K. K., Yuen, S., Lin, M. C., Kung, H. & Chiu, J. (2003).
       Serum biomarkers of hepatitis B virus infected liver inflammation: A
       proteomic study. *Proteomics* **3**, 666-674.

60. Yan, J. X., Wait, R., Berkelman, T., Harry, R. A., Westbrook, J. A., Wheeler, C. H. & Dunn, M. J. (2000). A modified silver staining protocol for visualization of proteins compatible with matrix-assisted laser desorption/ionization and electrospray ionisation-mass spectrometry. *Electrophoresis* **21**, 3666-3672.

61. Pramanik, R., Asplin, J. R., Lindeman, C., Favus, M. J., Bai, S. & Coe, F. L. (2004). Lipopolysaccharide negatively modulates vitamin D action by down-regulating expression of vitamin D-induced VDR in human monocytic THP-1 cells. *Cellular Immunology* **232**, 137-143.

62. Candiano, G., Bruschi, M., Musante, L., Santucci, L., Ghiggeri, G. M., Carnemolla, B., Orecchia, P., Zardi, L. & Righetti, P. G. (2004). Blue silver: a very sensitive colloidal Coomassie G-250 staining for proteome analysis. *Electrophoresis* **25**, 1327-1333.

63. Lewis, J. K., Wei, J. & Siuzdak, G. (2000). Matrix-assisted laser desorption/ionization mass spectrometry in peptide and protein analysis. In *Encyclopedia of Analytical Chemistry* (Meyers, R. A., ed.). John Wiley and Sons Ltd, Chichester.

64. Shevchenko, A., Wilm, M., Vorm, O. & Mann, M. (1996). Mass spectrometric sequencing of proteins from silver-stained polyacrylamide gels. *Analytical Chemistry* **68**, 850-858.

65. Hortin, G. L., Sviridov, D. & Anderson, N. L. (2008). High-abundance polypeptides of the human plasma proteome comprising the top 4 logs of polypeptide abundance. *Clinical Chemistry* **54**, 1608-1616.

66. Kitchin, F. D. & Bearn, A. G. (1966). The electrophoretic patterns of normal and variant phenotypes of the group specific (Gc) components in human serum. *American Journal of Human Genetics* **18**, 201-214.

67. Xue, X., Teare, M. D., Holen, I., Zhu, Y. M. & Woll, P. J. (2009). Optimizing the yield and utility of circulating cell-free DNA from plasma and serum. *Clinica Chimica Acta* **404**, 100-104.

6. Appendices

6.1   Buffers and solutions

6.1.1   Human β-defensin 2 (hBD-2) ELISA

Phosphate Buffered Saline (PBS)

8 g NaCl

0.25 g KCl

0.2 g KH_2PO_4

1.15 g Na_2HPO_4

Make up to 1L with dI water. Check pH is approx. 7.20 (7.0 – 7.4 is acceptable), and autoclave

Wash Buffer

0.05% Tween-20 in PBS

Make 1 L PBS and add 0.5 mL Tween-20. Check pH as above, and autoclave

Block Buffer

1% BSA in PBS

Store at 4 °C

Diluent

0.05% Tween-20, 0.1% BSA in PBS

Store at 4 °C

6.1.2   Tris-Tricine SDS-PAGE solutions

AB-3 (49.5% T, 3% C)

48 g acrylamide

1.5 g N, N'-methylenebisacrylamide

100 mL Milli-Q

AB-6 (49.5% T, 6% C)

46.5 g acrylamide

3 g N, N'-methylenebisacrylamide

100 mL Milli-Q

1x Anode Buffer (0.2 M Tris-Cl, pH 8.9)

24.22 g Tris base

500 mL water

Adjust to pH 8.9 with concentrated HCl

Dilute to 1 L with water

1x Cathode Buffer (0.1 M Tris, 0.1 M Tricine, 0.1 % (w/v) SDS)

12.11 g Tris base

17.92 g Tricine

1 g SDS

Dilute to 1 L with water

Tris-Cl/SDS, pH 8.45 (3.0 M Tris-Cl, 0.3 % SDS)   **(AKA Gel Buffer)**

182 g Tris base

300 mL water

Adjust pH to 8.45 with 1 N HCl

Dilute to 500 mL with water, and add 1.5 g SDS

Tricine Sample Buffer (0.1 M Tris, 24 % (w/v) glycerol, 8% (w/v) SDS, 0.2 M

DTT, 0.02 % (w/v) Coomassie Blue G-250)   **(AKA Gel Loading Buffer)**

2 mL 4x Tris-Cl/SDS, pH 6.8

 2.4 mL (3.0 g) glycerol

0.8 g SDS

0.3 g DTT

2 mg Coomassie Blue G-250

Add water to 10 mL and mix before making aliquots and storing at -20 °C

6.1.3   Laemmli gel solutions

30% acrylamide/0.8 % bisacrylamide

30 g acrylamide

0.8 g N, N'-methylenebisacrylamide

Add water to 100 mL total volume

Filter and store at 4 °C in the dark

4x Tris-Cl/SDS, pH 6.8 (0.5 M Tris-Cl, 0.4 % SDS)

Dissolve 6.05 g Tris base in 40 mL water. Adjust to pH 6.8 with 1N HCl. Add water to final volume of 100 mL. Filter and add 0.5 g SDS.

4x Tris-Cl/SDS, pH 8.8 (1.5 M Tris-Cl, 0.4% SDS)

Dissolve 91 g Tris base in 300 mL water. Adjust to pH 8.8 with 1N HCl. Add water to final volume of 500 mL. Filter and add 2 g SDS.

5x SDS electrophoresis buffer

7.55 g Tris base

36.0 g glycine

2.5 g SDS

Add water to 500 mL total volume, and dilute to a 1x working solution when appropriate.

2x SDS sample buffer

2.5 mL 4x Tris-Cl/SDS, pH 6.8

2.0 mL glycerol

0.4 g SDS

0.31 g DTT

Add water to 10 mL and mix, then store in aliquots at -20 °C.

6.1.4   Blue-silver staining solutions

Fixer (50 % methanol, 2% phosphoric acid)

250 mL methanol

10 mL phosphoric acid

Make up to 500 mL with water

Blue Micellar Solution

1.2 g Coomassie Blue G-250

100 g ammonium sulphate

200 mL methanol

100 mL phosphoric acid

700 mL water

Completely dissolve Coomassie in methanol before adding other ingredients, to prevent stain forming lumps in solution.

Destain (5% methanol)

25 mL methanol

475 mL water

6.1.5   Silver staining solutions

All silver staining solutions were made up in Milli-Q water

a) Basic silver saining

Fixer

50% ethanol

12% acetic acid

Sensitizer

0.02% sodium thiosulfate (2 mL 1% stock in 98 mL Milli-Q)

Stain

10 mL 1% silver nitrate stock

90 mL Milli-Q

100 μL 37% formaldehyde

Developer

100 mL 3% sodium carbonate

100 μL 37% formaldehyde

1 mL 1% sodium thiosulfate

b) He Silver Staining

Fixer

30% ethanol

10% acetic acid

Sensitizer

30% ethanol

4.1% sodium acetate

0.2% sodium thiosulfate

Stain

0.1% silver nitrate

0.02% formaldehyde

Developer

2.5% sodium carbonate

0.01% formaldehyde

c) Yan Silver Staining

Fixer

40% methanol

10% acetic acid

Sensitizer

30% methanol

0.2% sodium thiosulfate

6.8% sodium acetate

Stain

0.25% silver nitrate

Developer

2.5% sodium carbonate

0.04% formaldehyde

6.1.6   MALDI-TOF mass spectrometry

Calibration standard, CHCA and sDHB matrices, and targets were all purchased from Bruker Daltonics.

The peptide calibration standard contained the following peptides:

Angiotensin II, Angiotensin I, Substance P, Bombesin, ACTH clip 1-17,

ACTH clip 18-39, Somatostatin 28

6.1.7   DNA extraction from saline mouthwash

Lysis Solution

35 mL water

5 mL 1M Tris, pH 9.0

5 mL 0.5M EDTA

5 mL 10% SDS

1 mL 5M NaCl

6.1.8   PCR solutions

10x PCR Buffer

- 300mM Tris-HCl (pH 9.0)

- 300mM salts containing of K^+ and NH_4^+

- 20mM Mg^{2+}

- Enhancer solution

Master Mix

1 mL 10x PCR buffer (w/ 20mM $MgCl_2$)

1 mL dNTPs (2.5mM each)

8 mL water

iStarTaq polymerase (iNtRON) was used at 1.25U per 50 µL reaction

6x Loading Buffer

0.25% (w/v) bromophenol blue

0.25% (w/v) xylene cyanol FF

15% Ficoll (type 400)

Made up to desired volume with distilled water

50x Tris-acetate EDTA (TAE) buffer

242 g Tris base dissolved in 800 mL water

57.1 mL glacial acetic acid

100 mL 0.5 M EDTA (pH 8.0)

Make up to 1L with water

1x TAE running buffer

Dilute 20 mL 50x TAE stock with 980 mL water

2% Agarose/1xTAE gel with ethidium bromide

For one gel (approximately 30 mL):

0.6 g agarose

30 mL 1x TAE

Microwave until agarose is dissolved, then cool in a water bath before adding
3 µL 10 mg/mL ethidium bromide stock (1 µL per 10 mL agarose/TAE). Pour
into gel apparatus and leave to set.

6.2   PCR primer sequences

Common Forward:

5'-GGCATGTTTCACTTTCTGATCTC-3'

Wild-type Reverse:

5'-ACCAGCTTTGCCAGTACC**G**-3'

Mutant Reverse:

5'-GCAAAGTCTGAGTGCTTGTTATGCAGCTTTGCCAGTTGC**T**-3'

6.3   Vitamin D and ELISA results

6.3.1   Example calculation of peptide concentration

LL-37 and hBD-2 levels were determined from ELISA standard curves. The average absorbance of each duplicate set was used in the standard curve equation to give the peptide concentration. If the difference between the duplicate absorbance readings was greater than 15%, the ELISA for that sample was repeated. An example standard curve and dataset is shown below for hBD-2 ELISA.

Standard concentration (pg/mL)	Wavelength-corrected mean absorbance	Blank absorbance	Blank-corrected absorbance
1	0.2500	0.1154	0.1346
10	0.2603	0.1154	0.1449
100	0.7233	0.1154	0.6080
1000	1.3256	0.1154	1.2103

Standard curve generated by plotting standard concentration against blank- and wavelength-corrected mean absorbance:

Standard Curve

$$y = 923.03x^3 - 591.82x^2 + 198.07x - 9.083$$
$$R^2 = 1$$
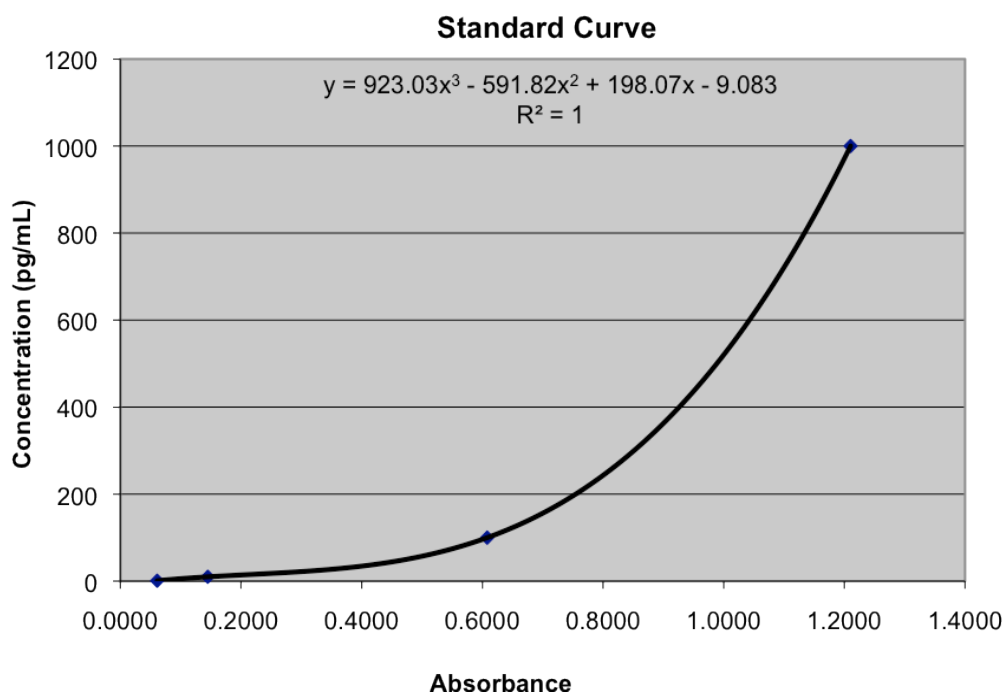
Example of ELISA data processing and calculation of plasma concentration

Raw data:

	Absorbance at 405 nm (after 30 min)	Absorbance at 690 nm
Blank	0.4809	0.3731
Blank (duplicate)	0.4929	0.3700
Mean	**0.4869**	**0.3716**
Percentage Difference	2.4646	0.8343

	Absorbance at 405 nm (after 30 min)	Absorbance at 690 nm
Sample 1	1.5257	0.8176
Sample 1 (duplicate)	1.5271	0.8204
Mean	**1.5264**	**0.8190**
Percentage Difference	0.0917	0.1834

Wavelength correction:

Corrected wavelength = Absorbance at 405 nm - Absorbance at 690 nm

i.e.   **Blank**   = 0.4869 - 0.3716

                    = 0.1153

        Sample 1   = 1.5264 - 0.8190

                    = 0.7074

Blank correction (to account for background effects):

Corrected wavelength = Sample absorbance - Blank absorbance

i.e.   = 0.7074 - 0.1153

                    = 0.5921

Determination of concentration:

The mean corrected absorbance is substituted in the place of x in the standard curve equation.

In this example:

$y = 923.03x^3 - 591.82x^2 + 198.07x - 9.083$ where $x = 0.5921$

Therefore, y = 92.29 pg/mL (bold and underlined in table below)

6.3.2 Raw vitamin D and ELISA results – CAP

Vitamin D level (ng/mL)	hBD-2 concentration (pg/mL)	LL-37 concentration (ng/mL)
74	840.99	83.42
48	590.31	82.58
22	-	263.49
69	205.61	156.88
37	103.35	87.3
79	426.1	35.2
66	608.28	189.59
60	779.87	100.29
110	-	-
62	**_92.29_**	21.85
34	79.42	88.83
71	54.62	159.03
55	207.64	72.89
25	187.07	165.59
64	256.77	45.73
42	378.13	79.67
48	-	-
12	494.5	36.38
90	233.95	30.35
97	283.21	63.28
39	1089.78	36.07
68	-	61.31
120	132.14	83.24
21	210.12	60.11
10	1467.25	147.87
38	40.93	60.31
48	1106.71	36.6
61	54.72	48.9
29	261.92	21.98
110	647.24	42.97
40	-	34.37
12	1228.25	101.87
74	201.19	38.81
77	1145.47	68.15
64	126.83	91.73
32	367.39	55.29
80	1002.35	72.28
45	47.79	112.26

58	-	-
38	978.91	64.85
25	260.36	210.64
46	680.84	166.98
51	1027.98	108.61
68	412.15	123.49
68	174.7	94.94
71	132.21	120.69
37	177.99	69.03
41	162.38	65.52
100	186.92	85.94
94	589.46	72.76
57	457.1	68.46
44	504.25	37.69
51	612.45	32.88
96	158.35	74.98
72	107.46	125.66
110	29.02	60.99
29	83.85	40.87
120	-	-
40	59.08	75.56
86	806.93	33.69
54	532.14	33.94
58	52.16	106.48
61	724.17	62.65
30	557.5	17.36
20	930.6	70.81
45	509.3	59.39
12	428.07	166
97	261.17	152.14
53	199.47	61.19
17	665.74	53.04
20	1061.75	47.76
33	148.45	73.26
73	219.35	120.2
59	215.19	85.37
67	-	201.45
45	-	-
56	522.58	112.13
35	1484.17	93.54
13	325.1	170.93
64	195.51	39.7
56	583.18	116.51
64	1642.04	-
81	302.14	49.48
100	449.82	13.16
82	-	-
40	77.78	65.69
39	31.02	63.96
66	518.95	46.72
47	174.75	87.83
51	106.4	191.44
49	178.63	44.06

60	258.64	152.55
26	115.17	20.72
57	285.35	84.68
73	13.96	22.18
58	47.87	25.98
56	-	-
33	242.17	69.42
61	437.81	61.1
53	1733.62	64.85
53	491.76	75.19
36	147.73	37.61
49	119.79	43.4
37	32.63	39.98
54	905.83	78.98
63	129.24	43.49
33	83.61	51.31
70	260.37	61.07
140	433.7	140.7
23	-	-
10	271.1	99.05
36	475.27	32.79

6.3.3 Raw vitamin D and ELISA results – COPD

Vitamin D level (ng/mL)	hBD-2 concentration (pg/mL)	LL-37 concentration (ng/mL)
26	154.25	73.17
54	298.24	98.6
64	136.82	59.99
37	166.91	49.75
13	332.11	52.93
56	112.14	67.09
50	148.8	44.99
48	86.34	54.79
89	96.04	49.38
70	1125.14	74.8
51	97.57	41.95
85	618.25	122.61
42	447.56	19.93
31	71.12	111.63
30	-	-
60	160.48	59.8
12	106.58	94.22
33	79.78	78.85
49	234.8	51.25
49	520.4	69.34
14	235.94	61
43	40.65	64.36
13	586.66	59.97
49	2469.39	35.97
24	77.18	10.26
42	63.9	131.66
73	-	97.65
41	146.98	60.13

35	236.52	55.51
40	17.69	93.78
10	-	88.31
58	333.6	101.36
65	77.49	31.63
32	1416.09	72.06
68	189.12	69.82
52	286.61	55.43
79	333.18	43.07
14	2006.72	66.64
42	420.83	55.58
32	24.23	62.31
49	15.31	40.91
10	303.23	30.13
51	188.38	341.25
81	74.37	68.38
66	232.31	40.13
52	-	-
39	256.01	77.62
35	213.96	18.37
57	117.08	68.59
43	68.55	29.69
19	88.42	75.99
49	150.39	35.85
62	564.17	29.2
26	1386.29	77.31
64	346.92	83.6
10	49.31	34.85
53	-	-
39	249.47	18.93
34	328.75	41.74
50	330.92	116.55
63	152.56	15.17
45	148.5	51.19
33	343.39	41.03
61	32.74	44.02
26	-	-
27	1366.35	66.07
63	50	96.9
30	194.56	65.47
62	718.41	108.34
54	80.2	93.64
65	541.17	23.51
12	81.3	50.62
71	39.7	48.06

6.4   Full results and spectra for MALDI hits

6.4.1   Expanded results for Table 3.3

i.   <u>Band 1</u>

- **Spectrum**
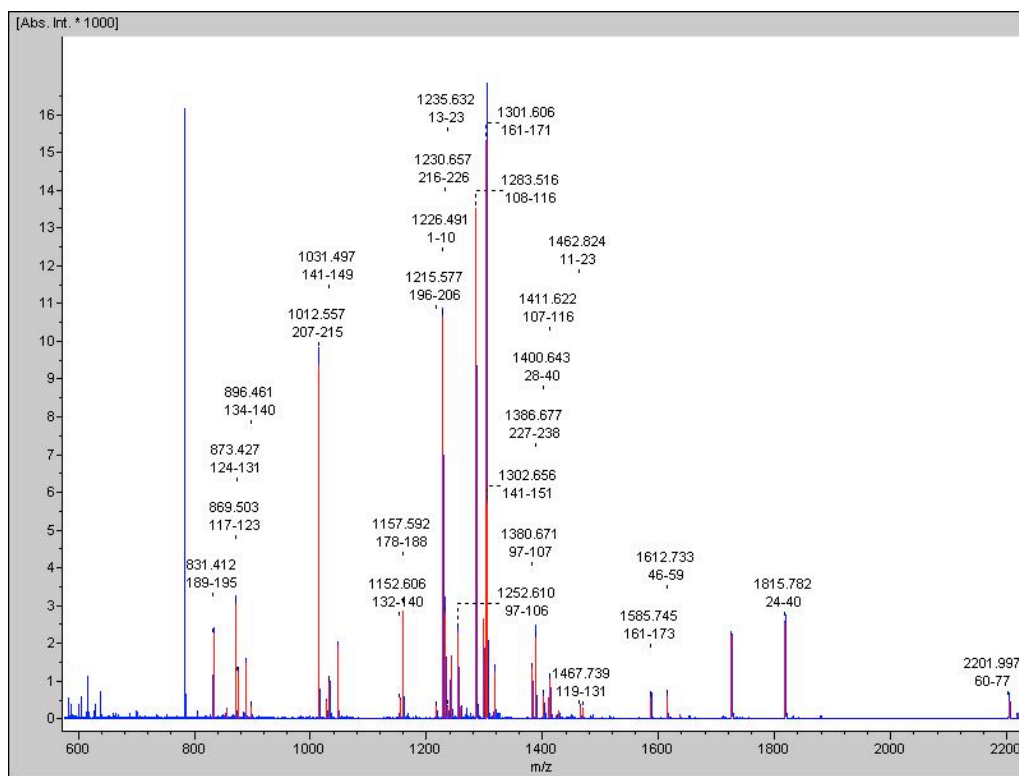
- **Peak list** (matches shown in **bold**)

m/z	SN	Quality Fac.	Res.	Intens.	Area
831.412	**91.5**	**1145**	**6699**	**2239.02**	**496**
853.411	9.9	612	6635	243.94	57
869.503	**121.5**	**1227**	**7146**	**3040.36**	**678**
873.427	**49.4**	**644**	**7639**	**1225.58**	**253**
887.442	57.5	733	7098	1467.42	308
896.461	**12.4**	**550**	**8340**	**313.36**	**62**
1012.557	388.1	6437	6808	9385.56	2730
1026.563	17.7	854	8497	461.85	115
1031.497	**37.8**	**700**	**8526**	**957.09**	**244**
1045.511	81.6	1036	6974	1901.06	539
1152.606	**25.6**	**860**	**5050**	**490.72**	**219**
1157.592	**154.9**	**5020**	**7512**	**3013.26**	**989**
1215.577	**9.5**	**974**	**7771**	**306.16**	**98**
1226.491	**310**	**45755**	**5324**	**10666.22**	**5589**
1230.657	**78.6**	**6481**	**5673**	**2797.55**	**1365**
1235.632	**8.8**	**442**	**5770**	**324.16**	**146**
1240.507	43.7	4819	5988	1638.97	748
1252.61	**57.6**	**8138**	**6267**	**2302.44**	**1001**
1257.594	8.3	584	6392	336.45	157
1283.516	**304.5**	**201975**	**5188**	**13557.84**	**7904**

1297.534	56.7	9325	5418	2650.78	1474
1301.606	**327**	**37872**	**4641**	**15354.88**	**10397**
1302.656	**121.3**	**649**	**4738**	**5712.52**	**3089**
1315.61	25	1876	6374	1241.01	636
1380.671	**47.4**	**6952**	**6127**	**1331.58**	**770**
1386.677	**82.2**	**7684**	**6772**	**2145.71**	**1166**
1400.643	**25.2**	**2559**	**6040**	**594.07**	**372**
1408.637	22.8	1387	5964	519.03	290
1411.622	**46.4**	**9971**	**5175**	**1041.61**	**675**
1425.62	10.2	493	5121	213.51	149
1462.824	**19**	**2031**	**5554**	**324.66**	**210**
1467.739	**15**	**1744**	**4862**	**249.89**	**195**
1585.745	**45.4**	**2752**	**5070**	**559.27**	**496**
1612.733	**47.9**	**4307**	**5708**	**593.34**	**516**
1634.686	7.6	744	6656	95.77	76
1723.891	166	3263	4102	2219.3	2878
1815.782	**223.3**	**3127**	**4070**	**2546.65**	**3641**
2201.997	**66.8**	**1448**	**3356**	**447.48**	**1020**
2215.958	17.2	1008	3403	99.16	244

- **Mascot search results**

Hit: **Chain A, Crystal Structure of Lipid-Free Human Apolipoprotein A-I**

Match to: **gi|90108664**

Score: **352**

Expect: **7.2e-30**

Nominal mass (M_r): **28061**

Calculated pI value: **5.27**

Taxonomy: *Homo sapiens*

Cleavage by Trypsin: cuts C-term side of KR unless next residue is P

Number of mass values searched: **39**

Number of mass values matched: **26**

Sequence Coverage: **82%**

ii.   **Band 2**

- **Spectrum**
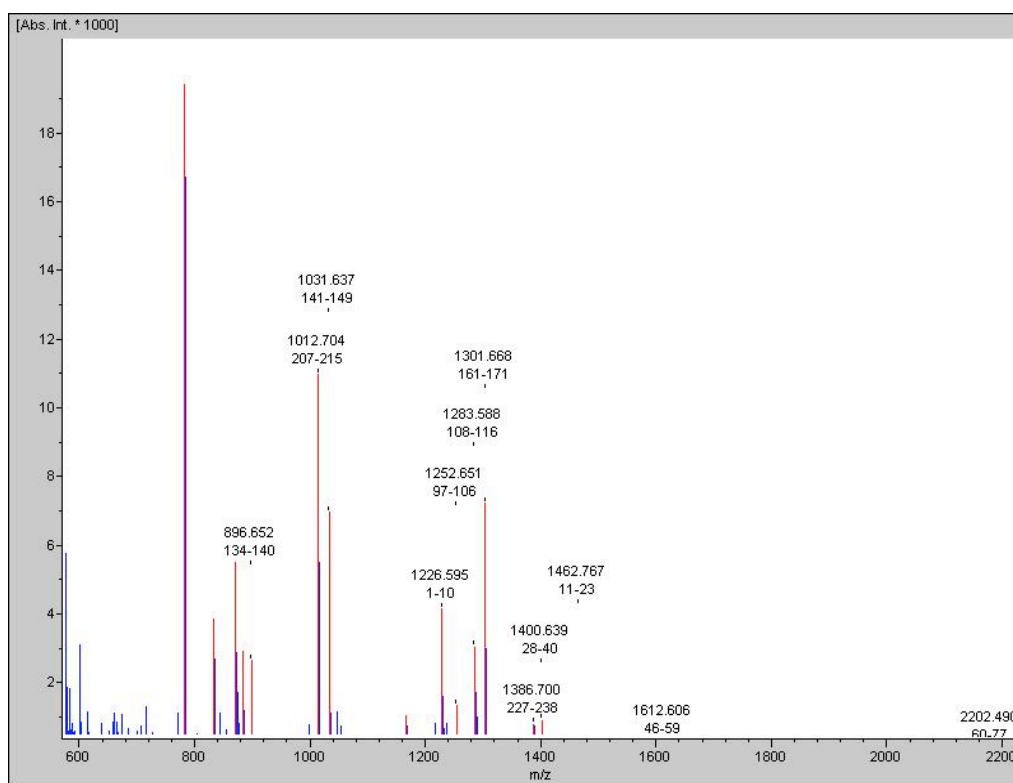
- **Peak list** (matches shown in **bold**)

m/z	SN	Quality Fac.	Res.	Intens.	Area
781.631	1283.9	1251616	5276	19429	3635
831.614	254.7	161482	6216	3855	655
869.699	364.2	339884	5980	5512	1052
882.738	192.3	150811	5744	2910	579
896.652	**174.8**	**112843**	**6636**	**2645**	**448**
1012.704	**730.6**	**529934**	**5769**	**11057**	**2385**
1031.637	**459.6**	**350165**	**5948**	**6955**	**1518**
1165.812	68.7	44572	5967	1039	281
1226.595	**279.3**	**213233**	**4197**	**4226**	**1416**
1252.651	**88**	**55691**	**5262**	**1332**	**402**
1283.588	**200.9**	**124933**	**3914**	**3041**	**1107**
1301.668	**477.4**	**289972**	**4144**	**7224**	**2603**
1386.7	**50.5**	**35622**	**5185**	**764**	**265**
1400.639	**59.2**	**37743**	**6214**	**896**	**266**
1448.865	22.3	14123	3918	338	145
1462.767	**9.3**	**4760**	**8417**	**140**	**33**
1562.836	6.1	3166	5758	92	32
1612.606	**16.9**	**11579**	**5987**	**255**	**92**
1677.58	7.9	4047	6849	120	38
1731.817	5.2	5007	5688	78	46
1812.685	8.6	2908	3634	130	58
1904.545	5.7	2217	4737	86	37
2202.49	**5**	**1391**	**6818**	**76**	**30**

- **Mascot search results**

Hit: **Chain A, Crystal Structure Of Lipid-Free Human Apolipoprotein A-I**

Match to: **gi|90108664**

Score: **155**

Expect: **2.4e-10**

Nominal mass (M_r): **28061**

Calculated pI value: **5.27**

Taxonomy: *Homo sapiens*

Cleavage by Trypsin: cuts C-term side of KR unless next residue is P

Number of mass values searched: **23**

Number of mass values matched: **12**

Sequence Coverage: **55%**

iv.   **Band 3**

- **Spectrum**
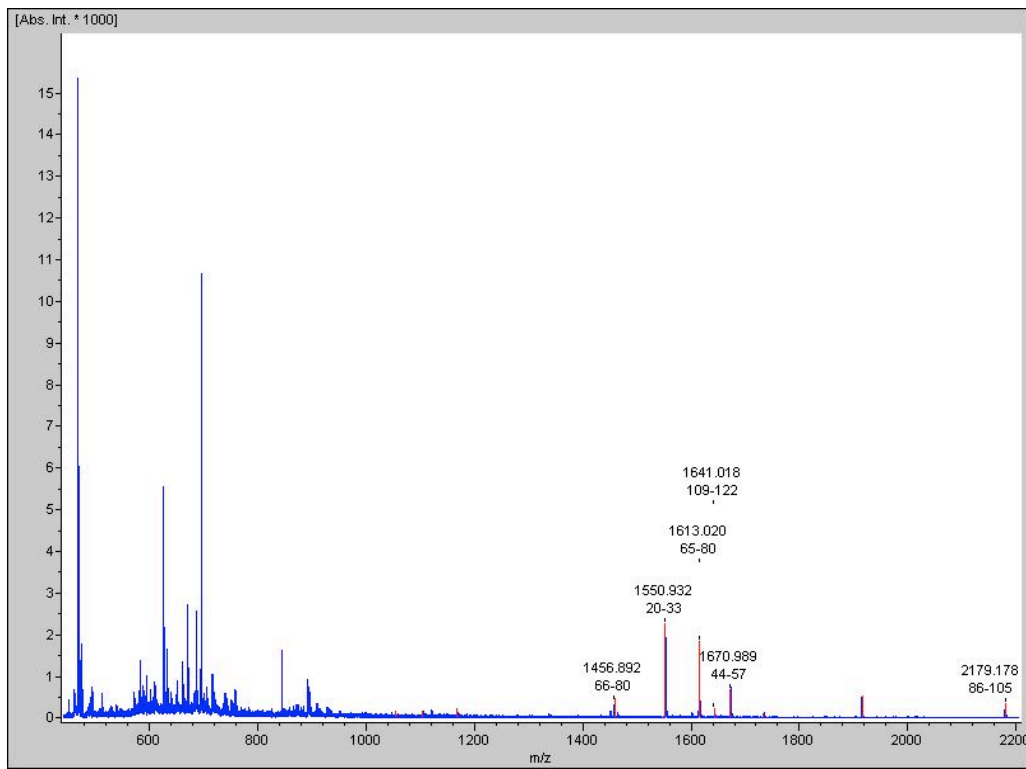
- **Peak list** (matches shown in **bold**)

m/z	SN	Quality Fac.	Res.	Intens.	Area
1051.806	9.1	6344	2462	155	75
1102.014	9	3449	5089	153	39
1165.886	14.1	12845	4717	241	91
1456.892	**27.5**	**21922**	**8014**	**469**	**125**
1550.932	**135.7**	**99727**	**6181**	**2311**	**736**
1613.02	**107.5**	**74479**	**6249**	**1832**	**601**
1641.018	**13.2**	**8694**	**7982**	**225**	**69**
1670.989	**43.8**	**27836**	**5858**	**746**	**248**
1732.341	6.3	3106	6826	108	36
1914.209	31.2	21281	6709	532	209
2179.178	**22.6**	**12575**	**6789**	**385**	**161**

- **Mascot search results**

Hit: **SAA1 protein [Homo sapiens]**

Match to: **gi|13937839**

Score: **110**

Expect: **7.6e-06**

Nominal mass (M_r): **13525**

Calculated pI value: **5.88**

Taxonomy: *Homo sapiens*

Cleavage by Trypsin: cuts C-term side of KR unless next residue is P

Number of mass values searched: **11**

Number of mass values matched: **6**

Sequence Coverage: **63%**

6.4.2   Expanded results for Table 3.6

i.   Band 1

- **Spectrum**
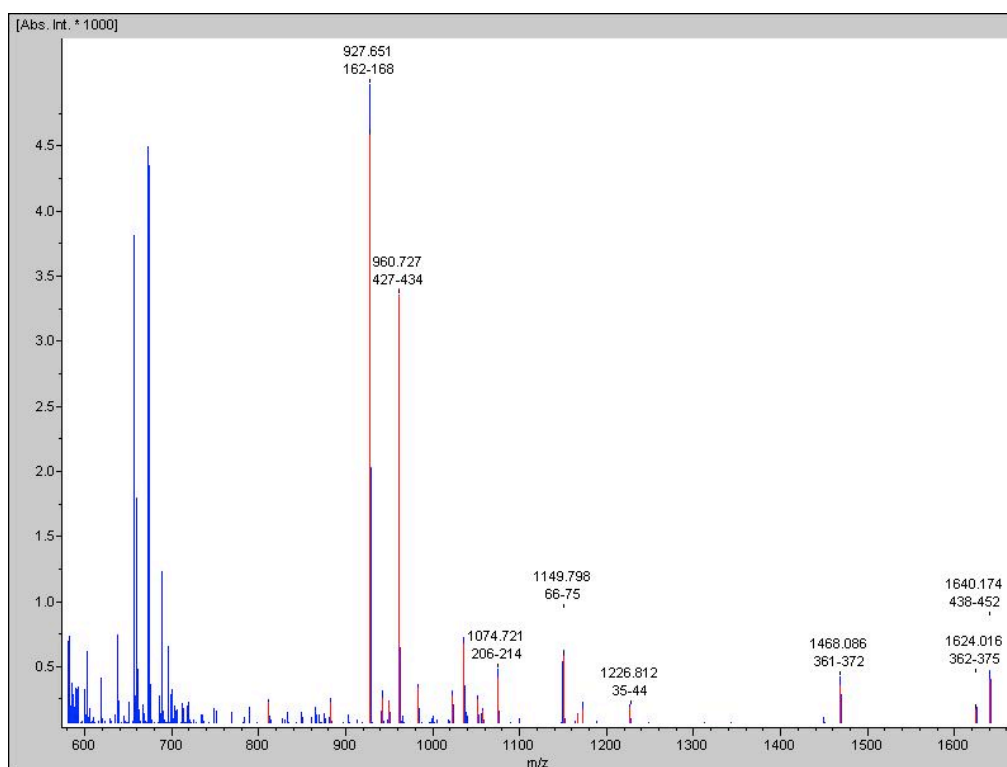
- **Peak list** (matches shown in **bold**)

m/z	SN	Quality Fac.	Res.	Intens.	Area
811.581	11	910	6232	224.47	50
882.719	10.8	477	8664	218.79	39
927.651	**237.4**	**6869**	**9299**	**4589.44**	**890**
941.654	13.2	442	8157	249.13	52
949.626	11.4	587	6197	217.15	54
960.727	**181.1**	**12844**	**8577**	**3402.86**	**696**
982.705	17.9	2031	8710	326.21	76
1022.75	16.1	428	7278	273.22	77
1035.747	39.2	2461	8588	667.88	153
1051.727	14.3	665	6891	236.06	75
1057.724	8.9	652	8222	150.7	37
1074.721	**25.1**	**1193**	**8397**	**404.93**	**95**
1149.798	**44.8**	**13168**	**7990**	**571.22**	**188**
1165.925	9.9	603	7473	126.08	38
1171.774	13	379	10906	158.85	44
1226.812	**16.1**	**1515**	**8044**	**177.05**	**59**
1468.086	**38.1**	**3486**	**7389**	**343.84**	**184**
1624.016	**19.3**	**1758**	**5965**	**165.15**	**127**
1640.174	**47.4**	**2046**	**5645**	**398.57**	**315**
1733.391	6.9	268	9615	44.42	30
2046.439	6.7	151	13318	32.64	29

- **Mascot search results**

Hit 1: **Albumin-like [Homo sapiens]**

Match to: **gi|763431**

Score: **91**

Expect: **0.0009**

Nominal mass (M_r): **52048**

Calculated pI value: **5.69**

Taxonomy: *Homo sapiens*

Cleavage by Trypsin: cuts C-term side of KR unless next residue is P

Number of mass values searched: **21**

Number of mass values matched: **8**

Sequence Coverage: **16%**

Hit 2: **Albumin, isoform CRA_t [Homo sapiens]**

Match to: **gi|119626083**

Score: **86**

Expect: **0.0027**

Nominal mass (M_r): **58614**

Calculated pI value: **6.66**

Taxonomy: *Homo sapiens*

Cleavage by Trypsin: cuts C-term side of KR unless next residue is P

Number of mass values searched: **21**

Number of mass values matched: **8**

Sequence Coverage: **14%**

Hit 3: **Chain A, Structure Of Human Serum Albumin With S-Naproxen And The Ga Module**

Match to: **gi|168988718**

Score: **86**

Expect: **0.0032**

Nominal mass (M_r): **65778**

Calculated pI value: **5.63**

Taxonomy: *Homo sapiens*

Cleavage by Trypsin: cuts C-term side of KR unless next residue is P

Number of mass values searched: **21**

Number of mass values matched: **8**

Sequence Coverage: **12%**

ii.   Band 2

- **Spectrum**
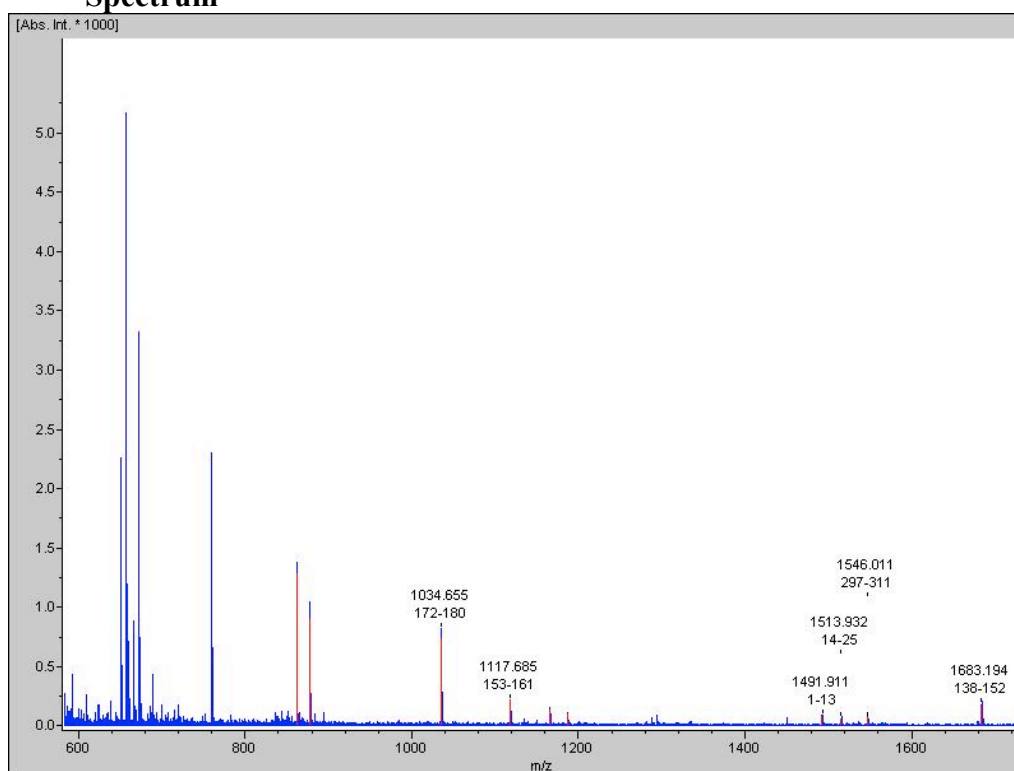
- **Peak list** (matches shown in **bold**)

m/z	SN	Quality Fac.	Res.	Intens.	Area
822.571	**44.2**	**1264**	**9343**	**1122.83**	**182**
836.563	**12.4**	**573**	**7178**	**336.53**	**69**
842.625	32.8	348	7617	919.23	184
844.607	**179.5**	**14521**	**6870**	**5079.87**	**1090**
858.604	11.2	330	4703	339.56	108
861.177	13	380	9448	405.81	61
864.613	10	275	8088	303.48	61
866.589	27.2	4691	6585	830.19	180
886.515	**18.1**	**269**	**8726**	**463.88**	**96**
980.582	**61.1**	**4450**	**8832**	**988.36**	**220**
1032.704	**144.7**	**24796**	**8202**	**2276.09**	**573**
1239.667	**18.2**	**1938**	**7290**	**203.88**	**84**
1552.846	13.2	1405	7754	115.46	67

- **Mascot search results**

Hit: **Fibrinogen beta chain, isoform CRA_f [Homo sapiens]**

Match to: **gi|119625340**

Score: **82**

Expect: **0.0064**

Nominal mass (M_r): **44153**

Calculated pI value: **8.84**

Taxonomy: _Homo sapiens_

Cleavage by Trypsin: cuts C-term side of KR unless next residue is P

Number of mass values searched: **13**

Number of mass values matched: **7**

Sequence Coverage: **13%**

iii.   <u>Band 3</u>

- **Spectrum**
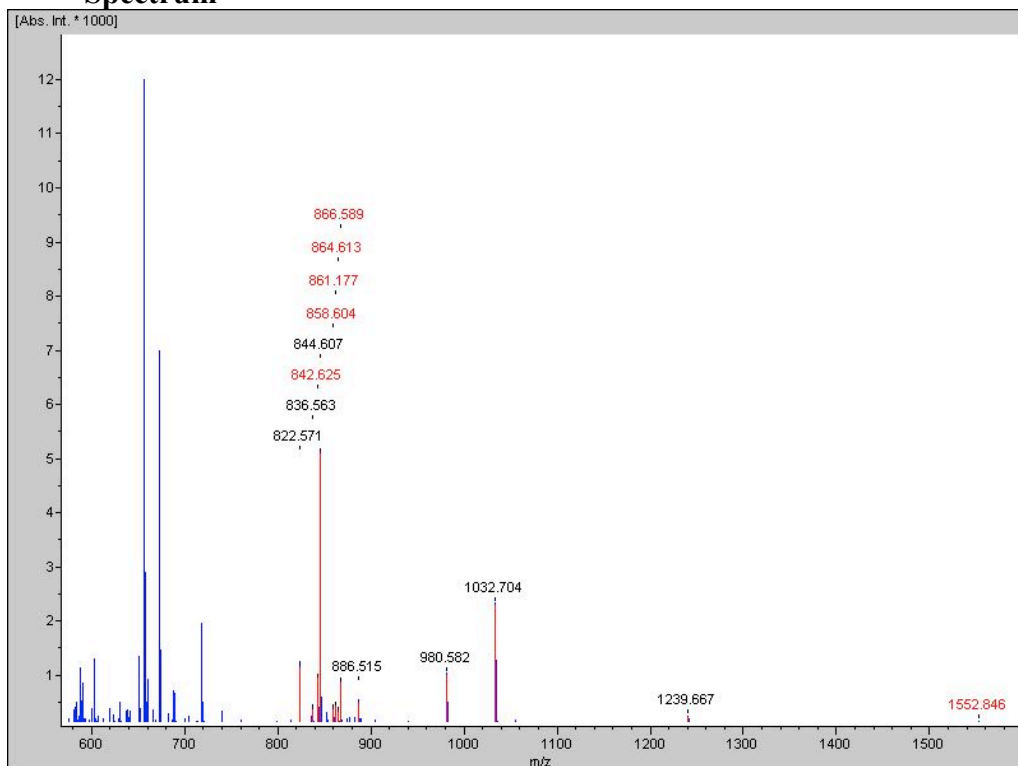
- **Peak list** (matches shown in **bold**)

m/z	SN	Quality Fac.	Res.	Intens.	Area
861.168	62.8	2535	6988	1282.66	252
877.145	47.7	1402	9345	902.01	167
1034.655	**60.1**	**3340**	**8636**	**741.67**	**177**
1117.685	**19.9**	**1369**	**7432**	**238.09**	**73**
1164.763	11.4	137	11919	131.61	36
1186.77	9	498	8119	96.91	28
1491.911	**10.4**	**786**	**7960**	**79.75**	**40**
1513.932	8.3	554	6790	63.13	39
1546.011	**9.1**	**820**	**6417**	**69.8**	**43**
1683.194	**24.7**	**1422**	**5118**	**169.11**	**150**
1873.21	25.2	574	5294	167.61	184

- **Mascot search results**

Hit: **Chain C, Crystal Structure Of Recombinant Human Fibrinogen Fragment D**

Match to: **gi|24987625** Score: **82** Expect: **0.0065**

Nominal mass (M_r): **35155**

Calculated pI value: **5.86**

Taxonomy: _Homo sapiens_

Cleavage by Trypsin: cuts C-term side of KR unless next residue is P

Number of mass values searched: **11**

Number of mass values matched: **6**

Sequence Coverage: **23%**

6.5   Sequencing results

Different combinations of the T436K and D432E genotypes produce the Gc isoforms, as indicated in Table 6.1.

Table 6.1 – Association between SNP alleles and Gc isoforms in DBP

Gc isoform	Alleles
Gc1S-1S	EE/TT
Gc1S-1F	DE/TT
Gc1F-1F	DD/TT
Gc1S-2	DE/TK
Gc1F-2	DD/TK
Gc2-2	DD/KK

The relevant part of exon 11, containing both SNP sites (underlined) is:

```
AAAATTGCC TGATGCCACA CCCACGGAAC TGGCAAAGCT GGTTAACAAG CACTCAGACT
           1                    2
```

Both SNPs trigger an amino acid substitution, as follows (changed nucleotide underlined):

D432E (site 1):
GAT = D allele (i.e. Aspartic acid)
GAG = E allele (i.e. Glutamic acid)

T436K (site 2):
ACG = T allele (i.e. Threonine)
AAG = K allele (i.e. Lysine)

The sequences of four individuals are included below, including the relevant section of each electropherogram. The codons responsible for determining the D432E and T436K alleles are underlined and in

bold. It should be noted that the poor sequencing results in the sample from lane 4 are expected, because this individual does not have a mutant allele.

### 6.5.1   Sequences and electropherograms – Multiplex protocol

From Figure 3.11 – **Lane 1**

```
ATTCATCACAGGTATAGATACTTAGGAGAAGGCAATAAAATATCCCCACCCCATCTAAAAGATCAG
AAACGGCTATTATTTTGCATTAGAAATTAGTATAAAATAAATACAAGTAGTAAGACCTTACATTTA
AAAGGTTTTTCAGACAGGCAGAGCGACTAAAAGCAAAATTGCCTGATGCCACACCCACGGTACAGC
AAAGCTGGTAGACAAGCATCAGACTTTGCATTTGCTTTTAGTCGCTCTGCGTCTGAATACATTTAA
TGTAGGTCTTCTACTGTAGTTATTTTATACAATTTCTAATGCAAATAATAGCTTTCGATCTTTTCA
TAAAATGAAAATGAAATACTTGCTGTCTCAGAAATTCTGTACTGTGGTATAGAAATCATTTGAGAT
CAAAATGAAACTGCCA
```
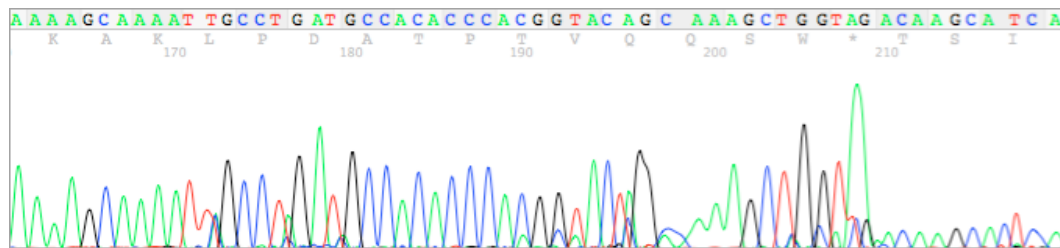

From Figure 3.11 – **Lane 2**

```
CGATCAAGGTTAGAATTTTCTTGAGACAGGCAAGTATTTCTATTTTCATTTTTATTGTAAAAGATC
TGAAATGGCTATTATTTTGCATTAGAAATTTGTATAAAATAAATACATGTAGTAAGACCTTACATT
TAAATGGTTTTTCAGACTGGCAGAGCGACTAAAAGCAAAATTGCCTGAGGCCACACCCACGGTACT
GAAAAGCTGGTTGAGTGGGTGTGGCTCAGCATTTTGCTTTTAGTCGCTCTGCGTCTGAAAACATTT
AATGTAGGTCTTACTACTGTATTTATTTTATACAATTTCTATGCAAATAATAGCTTTCGATCTTTT
CATAAAATGAAATGAAATACTTGCTGTCTCAGAAATTCTATACCTGTGGTATAGAAAGTCATTTGA
GATCAAAAATGAAACATGCCA
```
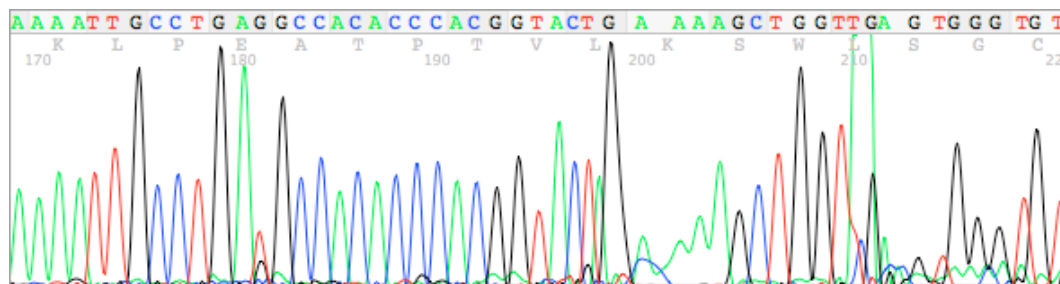
6.5.2 Sequences and electropherograms – Touchdown Protocol

From Figure 3.13 – **Lane 1 (Mutant Reverse)**

```
GATCATACACAGGTAAGATTTTCTTGAGACAGGCAAGTATTTCTATTTTCATTTTTATTGTAAAAG
ATCTGAAATGGCTATTATTTTGCATTAGAAATTTGTATAAAATAAATACATGTAGTAAGACCTTAC
ATTTAAATGGTTTTTCAGACTGGCAGAGCGACTAAAAGCAAAATTGCCTGATGCCACACCCAAGCA
ACAGGCAAAGCAGCATAACAAGCACACAGACTTTGC
```
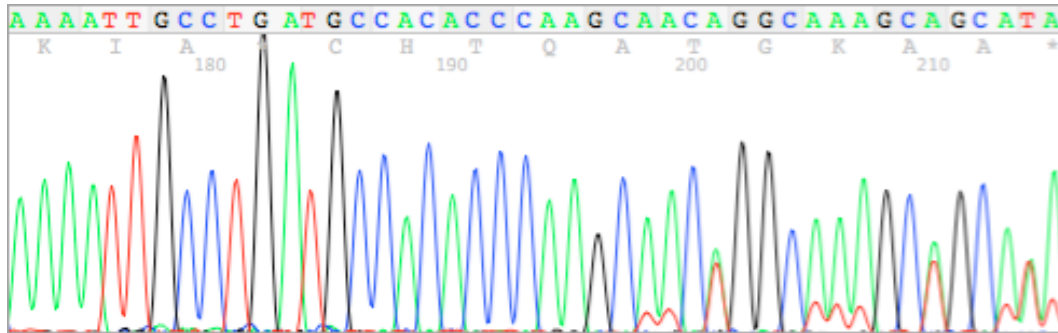

From Figure 3.13 – **Lane 2 (Wild-type Reverse)**

```
CAATTCAACACAGGTAAGATTTTCTTGAGACAGGCAAGTATTTCTATTTTCATTTTTATTGTAAAA
GATCTGAAATGGCTATTATTTTGCATTAGAAATTTGTATAAAATAAATACATGTAGTAAGACCTTA
CATTTAAATGGTTTTTCAGACTGGCAGAGCGACTAAAAGCAAAATTGCCTGAGGCCACACCCACGG
AACAGGCAAAGCAGGT
```
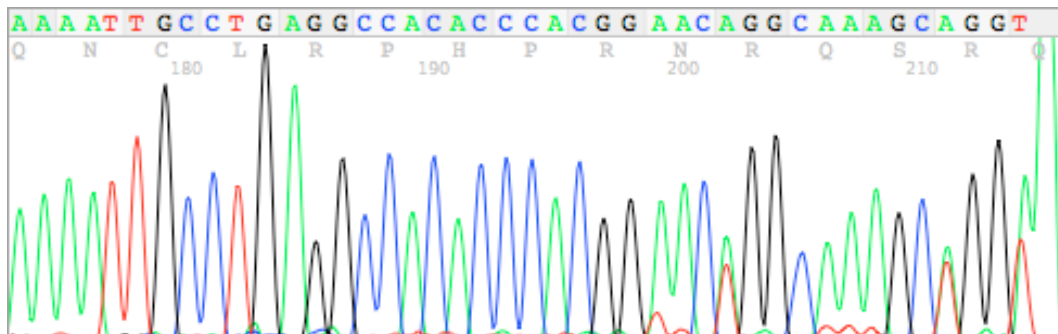

Note: The individual from lanes 1 and 2 therefore has the genotype DETK

From Figure 3.13 – **Lane 4 (Mutant Reverse)**

AAAGGGGGGGCGGTTGGGTTTGTAATCCGGGCGCAGACCTGGCTTTCTTGGGCTCGTTCGGCGGGGG
GTTAGGCGTCGGCTTGGCTGTCTAAAGGGGGTGAATGAGGTGGTGTGTAGCTTTTCTTAAAGGGGT
CACCGCGGAATTGCTGATCTGCTTTTATTGAGGGTCCGTTTCTCTGTATCGTGCGGTGACCC
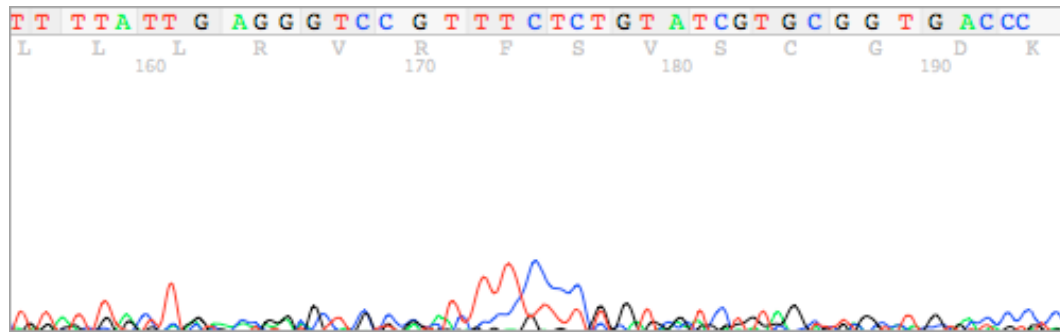
From Figure 3.13 – **Lane 5 (Wild-type Reverse)**

CATTCAAACACAGGTAAGATTTTCTTGAGACAGGCAAGTATTTCTATTTTCATTTTTATTGTAAAA
GATCTGAAATGGCTATTATTTTGCATTAGAAATTTGTATAAAATAAATACATGTAGTAAGACCTTA
CATTTAAATGGTTTTTTCAGACTGGCAGAGCGACTAAAAGCAAAATTGCCT**GAT**GCCACACCC**ACG**G
AACAGGCAAAGCAGGT
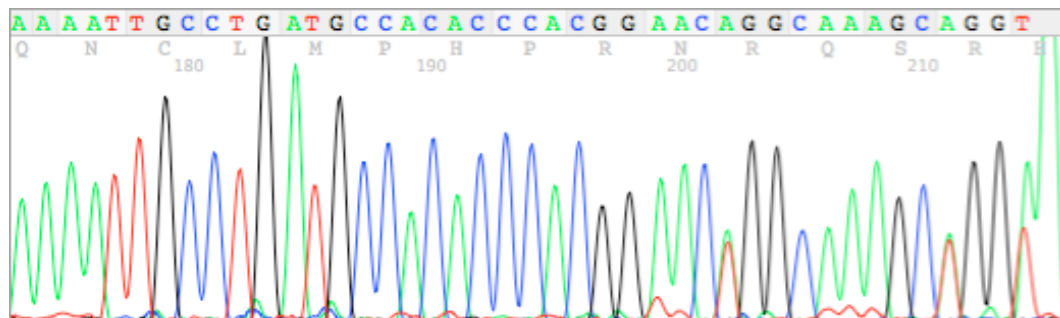
Note: *The individual from lanes 4 and 5 therefore has the genotype DDTT*